

AD-A031 293

MASSACHUSETTS INST OF TECH CAMBRIDGE DEPT OF OCEAN E--ETC F/G 13/10  
DETERMINATION OF DAMPING COEFFICIENTS OF SWATH CATAMARAN USING --ETC(U)  
JAN 75 K KIM

N00014-67-A-0204-0023

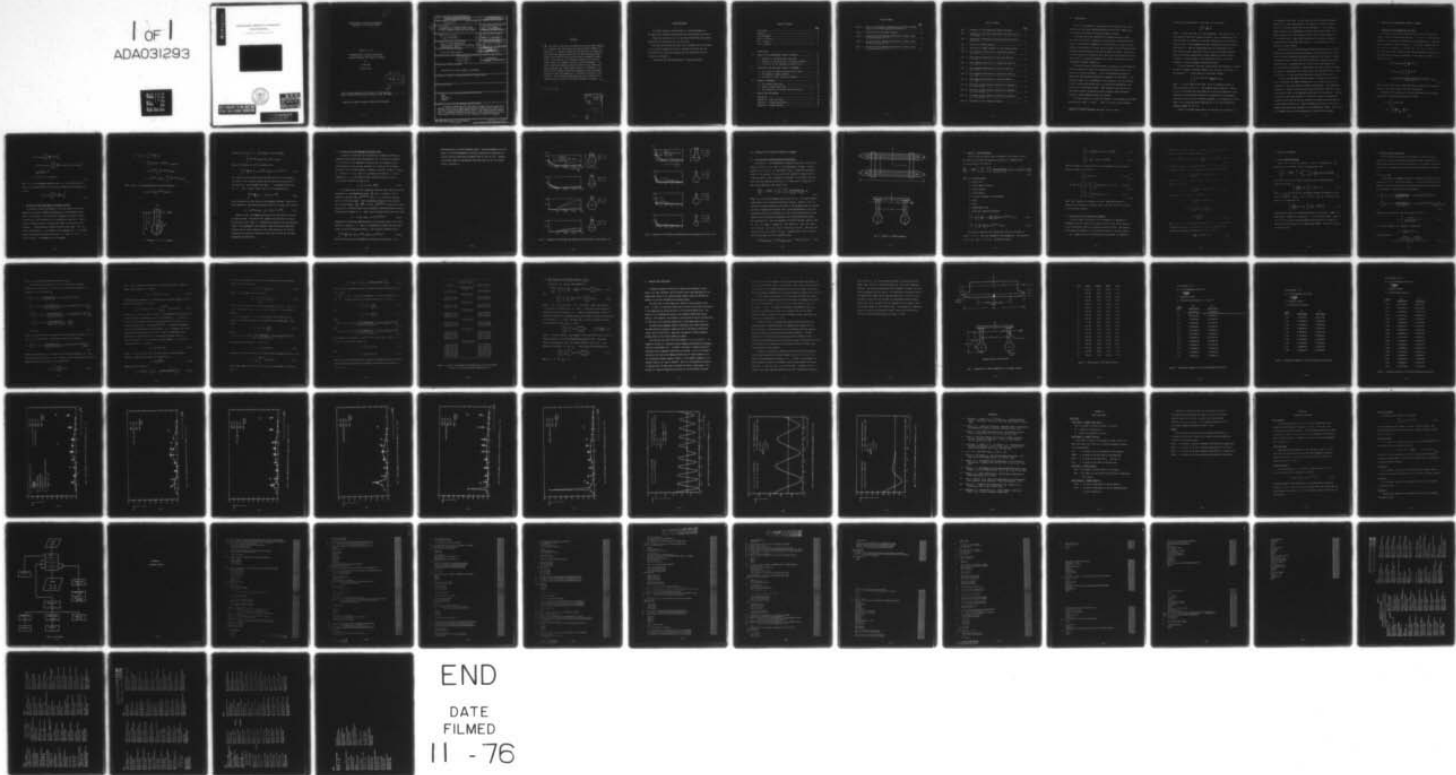
NL

UNCLASSIFIED

75-4

| OF |  
ADA031293

EFE  
EFC



END

DATE  
FILED

11 - 76



(1)

MASSACHUSETTS INSTITUTE OF TECHNOLOGY  
Department of Ocean Engineering

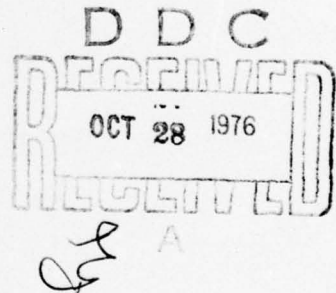
Report No. 75-4

DETERMINATION OF DAMPING COEFFICIENTS  
OF SWATH CATAMARAN USING THIN SHIP THEORY

by

Ki-Han Kim

January 1975



This work was supported by the Office of Naval Research,  
Contract N00014-67-A-0204-0023, NR 062-411, MIT OSP 70808. ✓ 220039

Approved for public release; distribution unlimited.

## SECURITY CLASSIFICATION OF THIS PAGE (When Data Entered)

REPORT DOCUMENTATION PAGE		READ INSTRUCTIONS BEFORE COMPLETING FORM
1. REPORT NUMBER <i>(14) 75-4</i>	2. GOVT ACCESSION NO.	3. RECIPIENT'S CATALOG NUMBER
4. TITLE (and Subtitle) DETERMINATION OF DAMPING COEFFICIENTS OF SWATH CATAMARAN USING THIN SHIP THEORY.		5. TYPE OF REPORT & PERIOD COVERED <i>(9) Final Report</i>
6. AUTHOR(s) <i>(10) Ki-Han Kim</i>	7. PERFORMING ORGANIZATION NAME AND ADDRESS Dept. of Ocean Engineering Massachusetts Institute of Technology Cambridge, Ma 02139	8. CONTRACT OR GRANT NUMBER(s) <i>(15) N00014-67-A-0204-0023</i>
9. CONTROLLING OFFICE NAME AND ADDRESS Office of Naval Research	10. PROGRAM ELEMENT, PROJECT, TASK AREA & WORK UNIT NUMBERS <i>(16) NR-062-H11 MIT-ASP-20808</i>	11. REPORT DATE <i>(11) January 1975</i>
12. NUMBER OF PAGES <i>(12) 78P.</i>	13. SECURITY CLASS. (of this report) Unclassified	14. DECLASSIFICATION/DOWNGRADING SCHEDULE
15. DISTRIBUTION STATEMENT (of this Report)  Distribution of this document is unlimited.		
16. DISTRIBUTION STATEMENT (of the abstract entered in Block 20, if different from Report)		
17. SUPPLEMENTARY NOTES		
18. KEY WORDS (Continue on reverse side if necessary and identify by block number) SWATH Ship Motion Damping		
19. ABSTRACT (Continue on reverse side if necessary and identify by block number)  A computer program has been developed to compute the pitch and heave damping coefficients of SWATH including forward speed effects based on the thin ship theory developed by Newman (1959). The results include comparisons of the damping coefficients with Lee's (1974) experiments for several Froude numbers and the effect of hull distance variations on damping.		

## ABSTRACT

This report deals with the problem of pitch and heave damping of a catamaran with small-waterplane-area-twin-hull (SWATH) configuration. A computer program has been developed to compute the pitch and heave damping coefficients of SWATH including forward speed effects based on the thin ship theory developed by Newman (1959). Calculations of the damping coefficients for several Froude numbers are compared with Lee's (1974) experiments. The results show that damping is greatly affected by the Brard parameter,  $\omega V/g$ , when the forward speed effects are considered. The effect of hull distance variation on damping is also considered. The results show that damping is an oscillatory function of hull distance. The oscillatory phenomenon dies out as the hull distance increases, and also as the Brard parameter increases.

$(\omega)(V)/g$

ACCESSION FOR	
#TIS	White Section <input checked="" type="checkbox"/>
DOC	Buff Sections <input type="checkbox"/>
ORIGINATOR	
IDENTIFICATION	
FURTHER AVAILABILITY CODES	
P.H. and/or SPECIAL	

A handwritten mark resembling a signature is written across the bottom of the form.

#### ACKNOWLEDGEMENTS

The author wishes to thank Professor J. Nicholas Newman for initiating this research and constantly give his guidance and advice.

Thanks are also due to Dr. K. June Bai without whose encouraging assistance this work would not have been done.

The author's gratitude also goes to Dr. Choung M. Lee of the NSRDC for his helpful suggestions and for providing the author with the experimental data which are compared with the theoretical results in Figures 6 through 11.

Discussions with Professor Ronald W. Yeung were helpful.

## TABLE OF CONTENTS

	<u>page</u>
Title Page.....	1
Abstract.....	2
Acknowledgement.....	3
Table of Contents.....	4
List of Tables.....	5
List of Figures.....	6
 I. INTRODUCTION.....	7
II. DAMPING OF TWO-DIMENSIONAL BULBOUS CYLINDERS.....	10
2.1 Damping of a Two-Dimensional Thin Body.....	10
2.2 Extension of Thin Ship Result to Bulbous Cylinder.....	11
2.3 Correction for the Submerged Cylindrical Part.....	14
III. EXTENSION OF THE THIN-SHIP THEORY TO CATAMARAN.....	18
3.1 The Interaction Effects Between the Two Hulls.....	18
3.2 The Damping of SWATH Catamaran.....	20
3.3 The Effects of Hull Distance on Damping.....	21
IV. NUMERICAL PROCEDURE.....	23
4.1 Zero Forward Speed Case.....	23
4.2 Nonzero Forward Speed Case.....	24
4.3 The Integration of the Hull Function ( $P_i, Q_i$ ).....	30
V. RESULTS AND DISCUSSIONS.....	31
References.....	48
Appendix A. Input and Output.....	49
Appendix B. Program Descriptions.....	51
Appendix C. Program Listing.....	54

## LIST OF TABLES

	<u>page</u>
Table 1. - Roots of the Legendre Polynomials $P_{n+1}(z)$ and the Weight Factors for the Gauss-Legendre Quadrature [1].....	29
Table 2. - Offset Data for the Sample Program.....	35
Table 3. - Theoretical Pitch Damping Coefficients of Large, Single and Twin Hulls at $F_n = 0.0$ .....	36
Table 4. - Theoretical Pitch Damping Coefficients of Large, Single and Twin Hulls at $F_n = 0.2$ .....	37
Table 5. - Theoretical Pitch Damping Coefficients of Large, Single and Twin Hulls at $F_n = 0.4$ .....	38

## LIST OF FIGURES

	<u>page</u>
Fig. 1 - Geometry of a Two-Dimensional Bulbous Cylinder.....	12
Fig. 2 - Comparison of Thin-Ship and Modified Thin-Ship Results with Frank's.....	16
Fig. 3 - Comparison of Thin-Ship and Modified Thin-Ship Results with Lee's.....	17
Fig. 4 - Geometry of SWATH Catamaran.....	19
Fig. 5 - Dimensions of SWATH Catamaran for the Sample Program.....	34
Fig. 6 - Heave Damping Coefficients of Single Hull MODCAT at $F_n = 0.0$ .....	39
Fig. 7 - Heave Damping Coefficients of Twin Hull MODCAT at $F_n = 0.0$ .....	40
Fig. 8 - Heave Damping Coefficients of Single Hull MODCAT at $F_n = 0.20$ .....	41
Fig. 9 - Heave Damping Coefficients of Twin Hull MODCAT at $F_n = 0.20$ .....	42
Fig. 10 - Heave Damping Coefficients of Single Hull MODCAT at $F_n = 0.40$ .....	43
Fig. 11 - Heave Damping Coefficients of Twin Hull MODCAT at $F_n = 0.40$ .....	44
Fig. 12 - The Effect of Hull Distance Variations on Damping at $F_n = 0.0 (\tau=0.0)$ .....	45
Fig. 13 - The Effect of Hull Distance Variations on Damping at $F_n = 0.05 (\tau=0.2)$ .....	46
Fig. 14 - The Effect of Hull Distance Variations on Damping at $F_n = 0.4 (\tau=1.6)$ .....	47
Fig. 15 - Flow Chart for the Computer Program.....	53

## I. INTRODUCTION

Due to the advantages of large deck area and stable motion characteristics in heavy seas, small-waterplane-area-twin-hull (SWATH) type of catamaran has become an interesting subject recently.

In recent work on the prediction of catamaran motions in waves, Lee (Pien and Lee [11]<sup>1</sup>) extended the strip-theory to catamaran configurations. A fundamental assumption in the strip-theory is that the hydrodynamic characteristics of a ship can be inferred from the two-dimensional stripwise characteristics of each section along the length. The effects of forward speed are included in Lee's work by the strip-theory synthesis rather than by a rigorous introduction of forward speed effects into the hydrodynamic boundary conditions.

The results based on the strip-theory are generally in good agreement with the experiments, except for a pronounced resonance effect in the theory at a critical frequency. At the corresponding wavelength the motions are substantially overpredicted compared with experiments. This resonance seems to be a consequence of the presence of near-zero damping at zero forward speed and the use of the zero-speed hydrodynamic coefficients in a strip-theory manner. This problem occurs only for hull forms where bulbous cylindrical sections, having a small waterplane area and a large submerged volume, are dominant.

To be more specific, let us first consider a two-dimensional thin-body section with a shape  $y = \pm h(z)$ . Then it is known that the damping

<sup>1</sup>Numbers in brackets designate Reference at end of paper.

coefficient is proportional to the square of the integral

$$\int_{-T}^0 e^{Kz} \frac{dh}{dz} dz$$

where  $T$  is the draft and  $K$  is the wavenumber. (See Section 2.1). It seems apparent that for a bulbous form where  $dh/dz$  changes sign, the above integral will vanish for a suitable combination of the wavenumber and hull shape. This phenomenon has been investigated earlier by Motora and Koyama [7]. They did experimental work on two-dimensional wave-excitationless forms, which have similar forms to the SWATH demi-hull. Frank [4] did some computations on heave damping for various bulbous cylinders. In both studies, it was shown that there is a critical frequency at which the damping coefficients vanish.

In three dimensions with zero forward speed, the situation is changed because the damping coefficient depends on an integral, with respect to the waveangle  $\theta$ , of the square of the surface integral

$$\int_{-L}^L \int_{-T}^0 e^{Kz + iKx \cos\theta} \frac{\partial h(x, z)}{\partial z} dz dx$$

where  $L$  is half length of the body. Since the damping integral is positive-definite for all  $\theta$ , zero-damping seems impossible. However, it can be anticipated that there might occur near-zero damping for long cylindrical vessels having essentially the appropriate two-dimensional form because there will be a dominant waveangle  $\frac{\pi}{2}$  as suggested by strip theory or the stationary phase approximation of the three-dimensional damping integral for  $KL \gg 1$ .

Finally, if forward speed effects are included, the possibility of

zero damping is even less. In this case, the three-dimensional damping coefficient is again proportional to the square of a surface integral similar to that shown above, but now the wavenumber  $K$  is no longer a single constant, but, depending on the value of the Brard number  $\omega V/g$ , takes on either two or four discrete values, each of which depends on  $\theta$  (See Newman [8]). Thus, since the square of the surface integral is integrated over a continuous spectrum of  $K$ , the probability of zero damping is greatly reduced.

Calculation of the three-dimensional damping coefficients, including forward speed effects without the assumption of strip theory is so complicated that some alternative simplifying assumptions are required. Newman [8] presented such a theory for "thin" mono-hulls, including illustrative calculations for a mathematical hull form for which experimental data had been obtained by Golovato. Subsequently, Gerritsma, Kerwin and Newman [5] presented comparisons of the same theory with experiments for a Series 60 hull form. In both cases the comparison was qualitatively useful.

In this report, Newman's thin-ship theory is applied to the catamaran hulls, especially with SWATH configuration, in an attempt to avoid the deficiency of the strip theory at nonzero forward speed. The fundamental assumption of Newman's thin-ship theory may be valid for these hull forms, since they are thin in the important region near the free surface. Moreover, to extend the practical validity of the present results, the submerged cylindrical hull portion will be treated by a modified thin-ship approach as described in Section 2.3. Based on Newman's work [8], pitch and heave damping coefficients are calculated for the NSRDC Model MODCAT. The results are compared with Lee's [6] experiments for various Froude numbers.

## II. DAMPING OF TWO-DIMENSIONAL BULBOUS CYLINDERS

### 2.1 Damping of a Two-Dimensional Thin Body

Consider a thin vertical body which is in an oscillatory heave motion on the free surface with velocity  $\zeta = V \cos \omega t$ . The fluid is assumed to be inviscid, irrotational and of infinite depth. Assume the body is symmetrical about the z-axis, z is positive upwards and its hull function is given by  $y = \pm h(z)$  for  $-T \leq z \leq 0$ , where T is the draft of the body. Then the velocity potential which satisfies the linearized free surface condition, in the region of positive y, is known to be [10]:

$$\begin{aligned} \phi &= 2e^{Kz} V \sin(Ky - \omega t) \int_{-T}^0 \frac{dh}{d\zeta} e^{K\zeta} d\zeta \\ &\quad - \frac{2}{\pi} V \cos \omega t \int_0^\infty \int_{-T}^0 \frac{dh}{d\zeta} e^{-ky} \\ &\quad \cdot \frac{(k \cos kz + K \sin kz)(k \cos k\zeta + K \sin k\zeta)}{k(k^2 + K^2)} d\zeta dk \end{aligned} \quad (2.1)$$

where the first term on the right hand side is related to the outgoing waves and the second term, to the local disturbance.

From Bernoulli's equation, the total hydrodynamic force acting on the body in z-direction is obtained as follows:

$$\begin{aligned} Z &= 2 \int_{-T}^0 p \cos(n, z) ds \\ &\stackrel{\sim}{=} -2 \int_{-T}^0 \left[ \frac{\partial \phi}{\partial t} \right]_{y=0} \frac{dh}{dz} dz \end{aligned}$$

$$\begin{aligned}
&= 4\omega\rho V \cos \omega t \left[ \int_{-T}^0 \frac{dh}{dz} e^{Kz} dz \right]^2 \\
&\quad - \frac{4}{\pi} \omega\rho V \sin \omega t \int_0^\infty \left[ \int_{-T}^0 \frac{dh}{dz} (k \cos kz + K \sin kz) dz \right]^2 \\
&\quad \cdot \frac{1}{k(k^2 + K^2)} dk \\
&\equiv b_{33} V \cos \omega t - a_{33} V \omega \sin \omega t
\end{aligned} \tag{2.2}$$

where  $b_{33}$  is the damping coefficient and  $a_{33}$  is the added mass coefficient. From the relation (2.2) we have a formula for the damping coefficient:

$$b_{33} = 4\omega\rho \left[ \int_{-T}^0 e^{Kz} \frac{dh}{dz} dz \right]^2 \tag{2.3}$$

## 2.2 Extension of Thin Ship Result to Bulbous Cylinder

As a means to check the validity of thin ship theory to find the damping coefficients of SWATH configurations, a two-dimensional model (Fig.1) is considered. In this section, damping of a heaving circular cylinder with a thin vertical strut is examined by using (2.3). Define a polar coordinate system  $(r, \theta)$  with the origin at the center of the cylinder,  $\theta$  being positive clockwise starting from z-axis. Let  $h(z)$  be the hull function,  $r_0$  the radius of the cylinder, and  $\theta_0$  the angle between z-axis and the bottom of the strut. If  $dh/dz = 0$  for  $z > -T + r_0(1 + \cos\theta_0)$ , the integral in (2.3) becomes:

$$\begin{aligned}
\int_{-T}^0 e^{Kz} \frac{dh}{dz} dz &= \int_{-T}^{-H} e^{Kz} \frac{dh}{dz} dz \\
&= \int_{\pi}^{\theta_0} e^{Kr_0} \cos \theta - K(T-r_0) r_0 \cos \theta d\theta \\
&= -r_0 e^{-KT_0} \int_{\theta_0}^{\pi} e^{Kr_0} \cos \theta \cos \theta d\theta \\
&= -r_0 e^{-KT_0} \{ \pi I_1(Kr_0) - \int_0^{\theta_0} e^{Kr_0} \cos \theta \cos \theta d\theta \}
\end{aligned} \tag{2.4}$$

where  $I_1(z)$  is the modified Bessel function defined by

$$I_1(z) = \frac{1}{\pi} \int_0^{\pi} e^z \cos \theta \cos \theta d\theta .$$

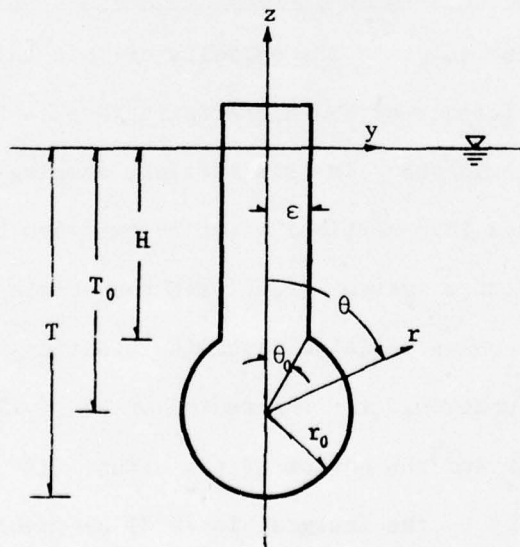


Fig. 1 Geometry of Bulbous Cylinder

Assuming  $Kr_0 \sin\theta_0 \ll 1$ , the integral in (2.4) becomes:

$$\int_0^{\theta_0} e^{Kr_0 \cos\theta} \cos\theta d\theta \approx \theta_0 e^{Kr_0} + O(\theta_0^2) .$$

Hence, the integral in (2.3) is reduced to be:

$$\int_{-T}^0 e^{Kz} \frac{dh}{dz} dz \approx -\pi r_0 e^{-KT_0} I_1(Kr_0) + \epsilon e^{-K(T_0 - r_0)} . \quad (2.5)$$

In a sense, the first term on the right hand side of (2.5) represents the effect of the circular cylinder and the second term, the effect of the thin strut. As an extreme case where  $\epsilon$  is negligibly small and  $Kr_0 \rightarrow 0$ , then  $I_1(Kr_0) \sim \frac{1}{2} Kr_0$  and (2.5) is approximated by:

$$\int_{-T}^0 e^{Kz} \frac{dh}{dz} dz \approx -\frac{1}{2} \pi r_0^2 K e^{-KT_0} \quad (2.6)$$

which represents only the effect of the submerged cylinder. Then the far field behavior of the velocity potential from (2.1), using (2.6), becomes:

$$\phi \approx 2V e^{Kz} \sin(Ky - \omega t) \left( -\frac{1}{2} \pi r_0^2 K e^{-KT_0} \right) \quad (2.7)$$

Based on (2.5), the damping coefficients are calculated for several cylindrical forms. The results are compared with Frank's [4] in Fig. 2 and with Lee's [6] in Fig. 3. Agreements are good for only low frequency range. Poor agreements in the frequency range of practical importance indicate that we need to modify the thin ship results for the circular cylindrical part which is actually not thin and for which the thin ship assumption may break down.

### 2.3 Correction for the Submerged Cylindrical Part

In order to account for the discrepancies in damping coefficients resulting from the thin ship approximation, Eqn. (2.5) will be modified for the effect of the submerged cylindrical part by comparing the far field behavior of the velocity potential (2.7) with that of the known solution of the circular cylinder. Consider a circular cylinder of radius  $r_0$  located at  $z = -T_0$  which is oscillating with velocity  $\zeta = V \cos \omega t$ . Assuming  $T_0 \gg r_0$  and using the same coordinate system as in Fig. 1, the velocity potential is known to be:

$$\phi = -V r_0^2 \cos \omega t \frac{\cos \theta}{r} \quad (2.8)$$

It is known (e.g. (13.31) in Wehausen & Laitone [13]) that the velocity potential of a two-dimensional source  $\frac{Q}{2\pi} \log r$  located at  $(0, -\zeta)$  behaves at infinity like  $Q e^{K(z+\zeta+iy)}$  where  $Q$  is the source strength and  $K$  is the wave number. The corresponding behavior of the potential of a vertical dipole  $\frac{Q}{2\pi} \frac{\cos \theta}{r}$  will be  $Q K e^{K(z+\zeta+iy)}$  since the velocity potential of a vertical dipole can be obtained by differentiating the source potential with respect to  $\zeta$ . Then it can be readily shown from (2.8) that:

$$\phi \sim -V r_0^2 \cos \omega t \cdot 2\pi K e^{K(z-T_0+iy)} \quad (2.9)$$

Comparing (2.9) with the limiting case of the thin ship result (2.7), they differ by a factor of 2. Thus it is reasonable to modify the thin ship results (2.5) by doubling the effect of the circular cylindrical part:

$$\int_{-T}^0 e^{Kz} \frac{dh}{dz} dz \approx -2\pi r_0 e^{-KT_0} I_1(Kr_0) + \epsilon e^{-K(T_0-r_0)} \quad (2.10)$$

Note that the last term is unmodified reflecting the importance of the

waterplane area in the low frequency limit. The same arguments will also apply to the three-dimensional case when we perform the integration of the hull function which has the similar form to that in (2.5). Damping coefficients based on the modified thin ship result (2.10) are plotted in Fig. 2 and Fig. 3.

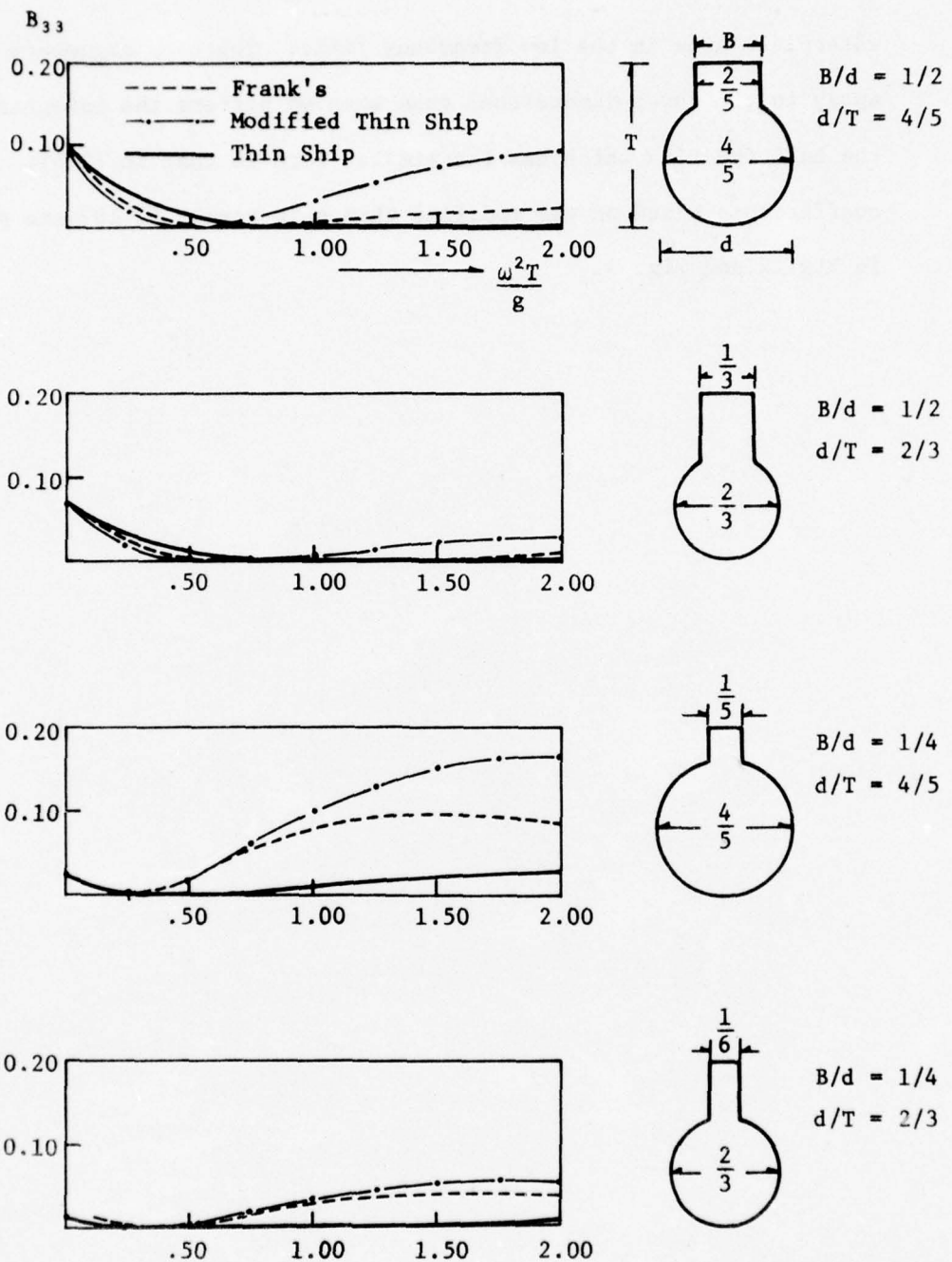


Fig. 2 Comparison of Thin-Ship and Modified Thin-Ship Results with Frank's [4]

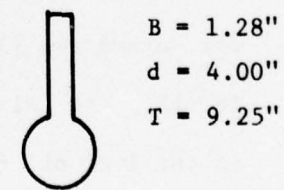
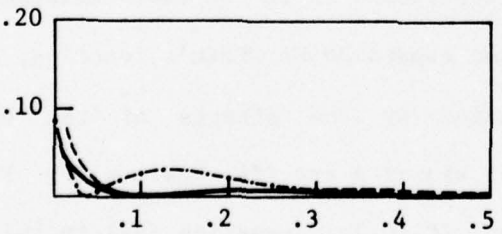
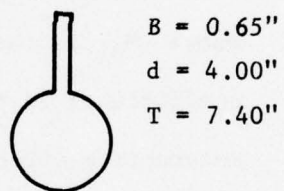
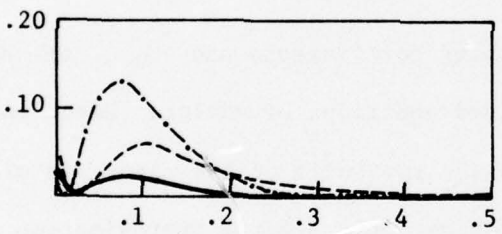
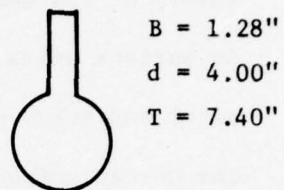
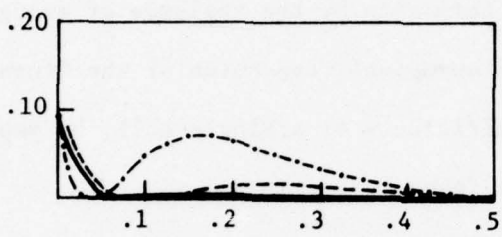
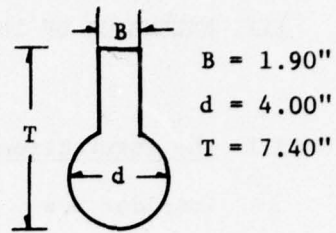
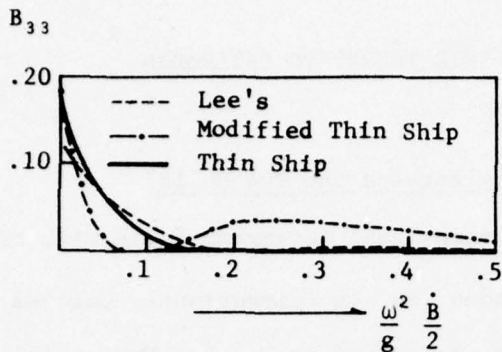


Fig. 3 Comparison of Thin-Ship and Modified Thin-Ship Results with Lee's [6]

### III. EXTENSION OF THE THIN-SHIP THEORY TO CATAMARAN

#### 3.1 The Interaction Effects Between the Two Hulls

Consider now three-dimensional catamaran hulls with cross sections having essentially the same as two-dimensional bulbous cylinders separated by a distance  $2b$  described in Fig.4. Newman [8] developed a theory of the damping of a thin ship by the analysis of energy radiation in surface waves. After an asymptotic expansion of the Green's function, pitch and heave damping coefficients of a single hull, by separation of the energy components, were found to be:

$$\begin{Bmatrix} M_q \\ Z_w \end{Bmatrix} = - \frac{2\rho\omega\nu\beta^2}{\pi} \int_{-\infty}^{\infty} \begin{Bmatrix} P_1^2 + Q_1^2 \\ P_2^2 + Q_2^2 \end{Bmatrix} \frac{(\tau K - 1)^4 \operatorname{sgn}(\tau K - 1)}{[(\tau K - 1)^4 - K^2]^{\frac{1}{2}}} dK \quad (3.1)$$

where  $M_q$  is the pitch damping coefficients and  $Z_w$ , the heave damping coefficients in the linearized equations of motion. Based on (3.1) the interaction effects between the two hulls of the catamaran will be included. In order to simplify the problem, only a first approximation to the hull interaction effects is considered; i.e. the source distributions of each separate hull are linearly superposed as in the wave-resistance theory for catamarans [3]. Then the expansion of Green's function, equation (66) in [8], is slightly changed by the effects of the twin hulls in the form of  $\{\exp(-i\lambda_i b \sin u) + \exp(i\lambda_i b \sin u)\}$ . Then the integration of the hull function  $(P_i, Q_i)$ , equation (69) in [8], is multiplied by the same factor for catamaran hulls:

$$(P_i, Q_i)_{\text{catamaran}} = (P_i, Q_i)_{\text{single hull}} \cdot 2 \cos(\lambda_i b \sin u) \quad (3.2)$$

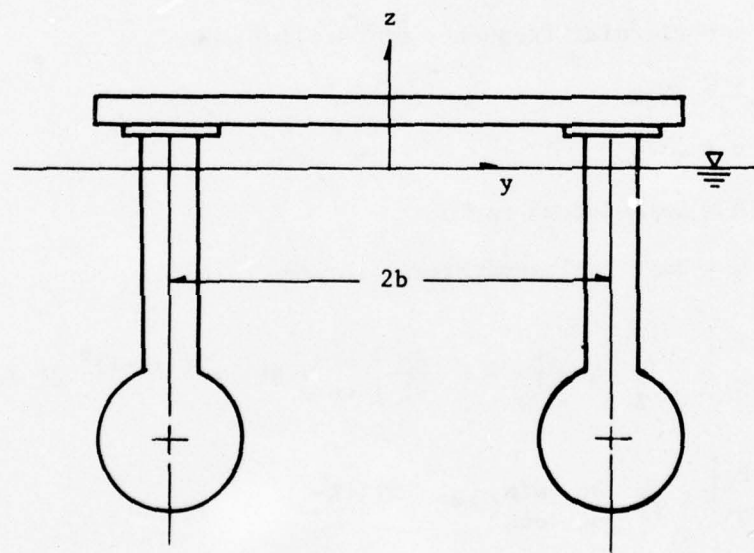
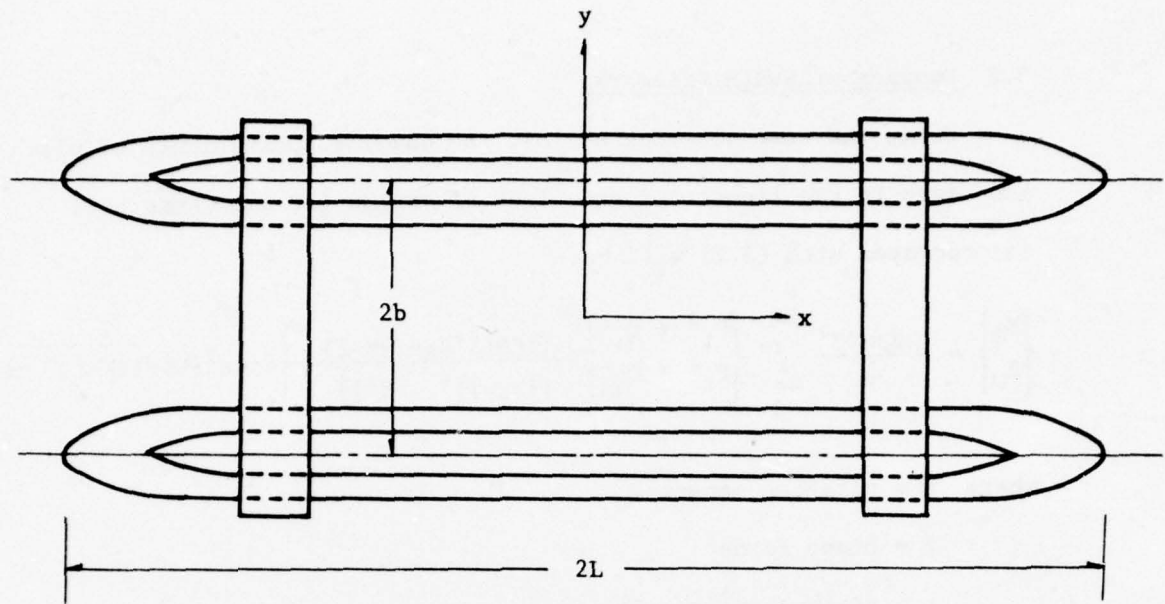


Fig. 4 Geometry of SWATH Catamaran

### 3.2 Damping of SWATH Catamaran

Using the same notation as [8], the damping coefficients of pitch and heave in the linearized equations of motion for catamaran hull incorporated with (3.2) will be:

$$\begin{Bmatrix} M_q \\ Z_w \end{Bmatrix} = -\frac{2\rho\omega\nu\beta^2}{\pi} \int_{-\infty}^{\infty} \begin{Bmatrix} P_1^2 + Q_1^2 \\ P_2^2 + Q_2^2 \end{Bmatrix} \cdot \frac{(\tau K-1)^4 \operatorname{sgn}(\tau K-1)}{[(\tau K-1)^4 - K^2]^{\frac{1}{2}}} \left\{ 4\cos^2[\nu b\sqrt{(\tau K-1)^4 - K^2}] \right\} dK \quad (3.3)$$

where  $M$  = pitching moment

$Z$  = heave force

$\nu$  = pitch angular velocity

$\omega$  = heave velocity

$\rho$  = fluid density

$\omega$  = circular frequency of oscillations

$\tau$  =  $\omega V/g$

$\nu$  =  $\omega^2/g$

$\beta$  = beam-length ratio

$b$  = half hull separation distance

$$\begin{Bmatrix} P_1 \\ Q_1 \end{Bmatrix} = \iint_S \left( \zeta \frac{\partial h}{\partial \xi} - \xi \frac{\partial h}{\partial \zeta} \right) \frac{\sin(\nu K \xi)}{\cos(\nu K \xi)} e^{\nu \zeta (\tau K - 1)^2} d\xi d\zeta \quad (3.4)$$

$$\begin{Bmatrix} P_2 \\ Q_2 \end{Bmatrix} = \iint_S \frac{\partial h}{\partial \zeta} \frac{\sin(\nu K \xi)}{\cos(\nu K \xi)} e^{\nu \zeta (\tau K - 1)^2} d\xi d\zeta \quad (3.5)$$

The prime in equation (3.3) denotes that only the intervals of  $(\tau K - 1)^4 - K^2 \geq 0$  are to be included in the integration. The intervals  $K_1 \leq K \leq K_2$  and  $K_3 \leq K \leq K_4$  are omitted, where

$$\left. \begin{array}{l} K_1 \\ K_2 \end{array} \right\} = Re \left\{ -\frac{1}{2\tau^2} [(2\tau-1) + (1-4\tau)^{\frac{1}{2}}] \right\} \quad (3.6)$$

$$\left. \begin{array}{l} K_3 \\ K_4 \end{array} \right\} = -\frac{1}{2\tau^2} [(2\tau+1) + (1+4\tau)^{\frac{1}{2}}] \quad (3.7)$$

Thus the integral in equation (3.3) can be decomposed in the following forms according to the values of  $\tau$  :

$$\int_{K_2}^{K_3} F(K) dK = I_1 \quad \text{if } \tau=0 \quad (3.8)$$

$$\int_{-\infty}^{\infty} F(K) dK = \left( \int_{-\infty}^{K_1} + \int_{K_2}^{K_3} + \int_{K_4}^{\infty} \right) F(K) dK = I_2 + I_3 + I_4 \quad \text{if } 0 < \tau < \frac{1}{4} \quad (3.9)$$

$$\left( \int_{-\infty}^{K_3} + \int_{K_4}^{\infty} \right) F(K) dK = I_5 + I_6 \quad \text{if } \tau > \frac{1}{4} \quad (3.10)$$

where  $F(K)$  denotes the integrand of (3.3). Numerical procedure to evaluate the integrals in equations (3.8), (3.9) and (3.10) are described in the subsequent chapter.

### 3.3 The Effects of Hull Distance on Damping

It can be easily anticipated that the damping of a catamaran is affected by the hull separation distance as well as the forward speed due to the interactions between the generated waves and hulls. The equation (3.3) shows that damping is an oscillatory function of the hull distance.

For a simple case of heave damping with zero speed, the asymptotic

behavior of the damping when  $b$  is large can be readily derived.

From (3.3), the heave damping integral when  $\tau=0$  is:

$$Z_w = - \frac{2\rho\omega v\beta^2}{\pi} \int_{-1}^1 (P_2^2 + Q_2^2) \frac{(-1)}{\sqrt{1-K^2}} 2[\cos(2vb\sqrt{1-K^2}) + 1] dK \quad (3.11)$$

In order to examine the asymptotic behavior of (3.11) for large  $b$ , consider only the oscillatory integral involving the cosine term:

$$I_1 \approx \int_{-1}^1 \frac{[P_2^2(K) + Q_2^2(K)]}{\sqrt{1-K^2}} \cos(2vb\sqrt{1-K^2}) dK \quad (3.12)$$

From (3.5),  $(P_2^2 + Q_2^2)$  can be shown to be an even function of  $K$ .

Then (3.12) becomes:

$$I_1 = 2 \int_0^1 \frac{(P_2^2 + Q_2^2)}{\sqrt{1-K^2}} \cos(2vb\sqrt{1-K^2}) dK \quad (3.13)$$

By a change of the variable,  $x = \sqrt{1-K^2}$ :

$$\begin{aligned} I_1 &= 2 \int_0^1 \frac{(P_2^2 + Q_2^2)}{\sqrt{1-x^2}} \cos(2vb\sqrt{x}) dx \\ &= 2 \int_0^1 \left\{ \frac{(P_2^2 + Q_2^2)}{\sqrt{1+x}} \right\} \frac{\cos(2vb\sqrt{x})}{\sqrt{1-x}} dx \\ &= 2 \int_0^1 f(x) \frac{\cos(2vb\sqrt{x})}{\sqrt{1-x}} dx \end{aligned} \quad (3.14)$$

where  $f(x)$  is a regular function between  $(0,1)$ . By a successive integration by parts (see Copson [2]), it can be shown that the leading order asymptotic behavior as  $b \rightarrow +\infty$  will be:

$$I_1 \sim \frac{1}{\sqrt{2vb}} \cos(2vb - \frac{\pi}{4}) \quad (3.15)$$

#### IV. NUMERICAL PROCEDURE

##### 4.1 Zero Forward Speed Case

When  $\tau=0$ ,  $K_2$  and  $K_3$  become -1 and +1 respectively. Thus equation (3.3) is reduced to the following simple form:

$$\begin{Bmatrix} M_q \\ Z_w \end{Bmatrix} = -\frac{2\rho\omega\nu\beta^2}{\pi} \int_{-1}^{+1} dK \begin{Bmatrix} P_1^2 + Q_1^2 \\ P_2^2 + Q_2^2 \end{Bmatrix} \frac{(-1)}{\sqrt{1-K^2}} \left\{ 4\cos^2[\nu b\sqrt{1-K^2}] \right\} \quad (4.1)$$

The integral in (4.1) is easily evaluated using the Gauss-Chebyshev quadrature formula:

$$\int_{-1}^{+1} \frac{F(K)}{\sqrt{1-K^2}} dK = \sum_{i=1}^m w_i F(K_i) + E_n \quad (4.2)$$

where  $K_i$  are the roots of the  $m^{\text{th}}$ -degree Chebyshev polynomial, so that  $K_i = \cos \frac{(2i-1)\pi}{2m}$ ,  $i=1, 2, \dots, m$ ;  $w_i = \pi/m$ ; and  $E_n$  is an error term.

Then (4.2) is simplified to:

$$\int_{-1}^{+1} \frac{F(K)}{\sqrt{1-K^2}} dK = \frac{\pi}{m} \sum_{i=1}^m F \left\{ \cos \frac{2(i-1)\pi}{2m} \right\} \quad (4.3)$$

Damping coefficients are non-dimensionalized by the quantity  $\rho\nu\sqrt{g/L}$  for heave and by  $\rho\nu L\sqrt{g/L}$  for pitch where  $\nu$  is a displaced volume. Based on (4.1) and (4.3), pitch and heave damping coefficients for a single and twin hulls are calculated for the NSRDC model MODCAT. Results are plotted in Fig.6 and Fig.7.

#### 4.2 Nonzero Forward Speed Case

If the forward speed effects are included, not only the finite integral but also the semi-infinite integrals should be evaluated. The semi-infinite integrals are quite involved due to the highly oscillatory cosine term. Consider the two cases separately according to the values of  $\tau$ .

$$(a) \quad 0 < \tau < 1/4$$

In this case, the damping integral is decomposed in three different ranges as in (3.9). The finite integral  $I_3$  can be treated in the same manner as the zero speed case by an appropriate change of the variable of the integration. Rewriting the finite integral:

$$\begin{aligned} I_3 &= \int_{K_2}^{K_3} (P_i^2 + Q_i^2) \frac{(\tau K - 1)^4 \operatorname{sgn}(\tau K - 1)}{\sqrt{(\tau K - 1)^4 - K^2}} \cdot 4 \cos^2 [\sqrt{b} \sqrt{(\tau K - 1)^4 - K^2}] dK \\ &= \int_{K_2}^{K_3} \left\{ (P_i^2 + Q_i^2) \frac{(\tau K - 1)^4 \operatorname{sgn}(\tau K - 1)}{\tau^2 \sqrt{(K_4 - K)(K - K_1)}} \cdot 4 \cos^2 [\sqrt{b} \sqrt{(\tau K - 1)^4 - K^2}] \right\} \frac{dK}{\sqrt{(K - K_2)(K_3 - K)}} \end{aligned} \quad (4.4)$$

Denoting the expression in the braces above by  $F_3(K)$ ,

$$I_3 = \int_{K_2}^{K_3} \frac{F_3(K)}{\sqrt{(K - K_2)(K_3 - K)}} dK \quad (4.5)$$

By a linear change of the variable of integration,

$$x = \frac{2}{K_3 - K_2} (K - K_3) + 1$$

(4.5) reduces to:

$$I_3 = \int_{-1}^1 \frac{F_3 \left\{ \left( \frac{K_3 - K_2}{2} \right) x + \left( \frac{K_3 + K_2}{2} \right) \right\}}{\sqrt{1 - x^2}} dx \quad (4.6)$$

where we can use Gauss-Chebyshev quadrature formula.

The semi-infinite integrals in (3.9) and (3.10) can be treated essentially in the same way. In order to facilitate the integrals, we manipulate in the following way:

$$\begin{aligned}
 I_2 &= \int_{-\infty}^{K_1} (P_1^2 + Q_1^2) \frac{(\tau K - 1)^4 \operatorname{sgn}(\tau K - 1)}{\sqrt{(\tau K - 1)^4 - K^2}} \cdot 4 \cos^2 [\nu b \sqrt{(\tau K - 1)^4 - K^2}] dK \\
 &= \int_{-\infty}^{K_1} (P_1^2 + Q_1^2) \frac{(\tau K - 1)^4 \operatorname{sgn}(\tau K - 1)}{\tau^2 \sqrt{(K_4 - K)(K_3 - K)(K_2 - K)}} \cdot 2[\cos(2\nu b \sqrt{(\tau K - 1)^4 - K^2}) + 1] \frac{dK}{\sqrt{K_1 - K}} \\
 &= 2 \int_{-\infty}^{K_1} \left\{ (P_1^2 + Q_1^2) \frac{(\tau K - 1)^4 \operatorname{sgn}(\tau K - 1)}{\tau^2 \sqrt{(K_4 - K)(K_3 - K)(K_2 - K)}} \cdot \cos[2\nu b \sqrt{(\tau K - 1)^4 - K^2}] \right\} \frac{dK}{\sqrt{K_1 - K}} \\
 &\quad + 2 \int_{-\infty}^{K_1} (P_1^2 + Q_1^2) \frac{(\tau K - 1)^4 \operatorname{sgn}(\tau K - 1)}{\tau^2 \sqrt{(K_4 - K)(K_3 - K)(K_2 - K)}} \frac{dK}{\sqrt{K_1 - K}} \\
 &= 2(I_a + I_b) \tag{4.7}
 \end{aligned}$$

where  $I_a$  denotes the first integral with an oscillatory integrand in (4.7) and  $I_b$ , the second one. Concerning only the first integral,

$$I_a = \int_{-\infty}^{K_1} \left\{ (P_1^2 + Q_1^2) \frac{(\tau K - 1)^4 \operatorname{sgn}(\tau K - 1)}{\tau^2 \sqrt{(K_4 - K)(K_3 - K)(K_2 - K)}} \cos[2\nu b \sqrt{(\tau K - 1)^4 - K^2}] \right\} \frac{dK}{\sqrt{K_1 - K}} \tag{4.8}$$

Dominant contributions to the integral come from the vicinity of  $K_1$  since the oscillations get faster as  $|K|$  increases, thus cancelling out effectively.

Equation (4.8) can be written in the simple form:

$$I_a = \int_{-\infty}^{K_1} \frac{F_2(K)}{\sqrt{K_1 - K}} dK \tag{4.9}$$

where  $F_2(K)$  denotes the expression in the braces in (4.8). Then by a change of the variable,  $x = \sqrt{K_1 - K}$ :

$$I_a = 2 \int_0^\infty F_2(K_1 - x^2) dx \quad (4.10)$$

The semi-infinite integral is subdivided into an infinite number of finite ones of an interval  $A$ , so that:

$$I_a = 2 \int_0^\infty F_2(K_1 - x^2) dx = 2 \sum_{n=0}^{\infty} \int_{A_n}^{A(n+1)} F_2(K_1 - x^2) dx \quad (4.11)$$

However, due to the oscillatory nature of the integrand in (4.8), we should be very careful in choosing the size of the interval  $A$ . In order to account for the change in period of an oscillation, the interval  $A$  is chosen as the period of  $\cos(2\sqrt{b}\sqrt{(\tau K_1)^2 - K^2})$ . Then the sub-integrals in (4.11) are performed over these periods. As  $n$  increases, the contribution of the sub-integral gets smaller. Thus the integration can be performed to a desired accuracy by controlling the upper limit of  $n$ .

After the value of  $A$  is determined, the sub-integral  $I_1$  in (4.11) for a given value of  $n$ , becomes:

$$I_1 = \int_a^b F_2(K_1 - x^2) dx \quad (4.12)$$

where  $a$  and  $b$  are the lower and upper limits of the sub-interval.

Then by a change of the variable of integration to:

$$z = \frac{2x - (a+b)}{b - a} \quad (4.13)$$

Equation (4.12) reduces to:

$$I_1 = \frac{b-a}{2} \int_{-1}^1 F_2 \left\{ K_1 - \left[ \frac{z(b-a) + (a+b)}{2} \right]^2 \right\} dz \quad (4.14)$$

We now have an appropriate integral form for which we can use the Gauss-Legendre quadrature formula:

$$\int_{-1}^1 F(z) dz \approx \sum_{i=0}^n w_i F(z_i) \quad (4.15)$$

where  $w_i$  are weight factors given by:

$$w_i = \int_{-1}^1 \prod_{\substack{j=0 \\ j \neq i}}^n \left[ \frac{z - z_j}{z_i - z_j} \right] dz \quad (4.16)$$

and  $z_i$  are the roots of the Legendre Polynomial  $P_{n+1}(z)$ . The roots  $z_i$  and the weight factors  $w_i$  for several values of  $n$  are listed in Table 1.

For the integral  $I_4$ , the same procedure can be used as in  $I_2$  except for a different change of the variable of the integration. From (3.9),

$$I_4 = \int_{K_4}^{\infty} F_4(K) \frac{dK}{\sqrt{K-K_4}} \quad (4.17)$$

where

$$F_4(K) = (P_i^2 + Q_i^2) \left\{ \frac{(\tau K - 1)^4 \operatorname{sgn}(\tau K - 1)}{\tau^2 \sqrt{(K - K_1)(K - K_2)(K - K_3)}} \right\} \left\{ 4 \cos^2 \left[ \sqrt{\tau b} \sqrt{(\tau K - 1)^4 - K^2} \right] \right\}$$

By changing of the variable,  $x = \sqrt{K - K_4}$ :

$$I_4 = 2 \int_0^{\infty} F_4(K_4 + x^2) dx \quad (4.18)$$

Analogous to (4.11), we subdivide the semi-infinite integral into finite ones:

$$I_4 = 2 \sum_{n=0}^{\infty} \frac{A(n+1)}{A_n} \int_0^{\infty} F_4(K_4 + x^2) dx \quad (4.19)$$

By the same change of the variable (4.13), each sub-integral in (4.19) reduces to:

$$I_1 = \frac{b-a}{2} \int_{-1}^1 F_4 \left\{ K_4 + \left[ \frac{z(b-a) + (a+b)}{2} \right]^2 \right\} dz \quad (4.20)$$

where the Gauss-Legendre quadrature formula (4.15) and (4.16) may be used.

(b)  $\tau > 1/4$

When  $\tau > 1/4$ , we have two integrals  $I_5$  and  $I_6$  similar to  $I_2$  and  $I_4$ . Briefly repeating the same procedure as in  $I_2$  and  $I_4$ :

$$I_5 = \int_{-\infty}^{K_3} F_5(K) \frac{dK}{\sqrt{K_3 - K}} \quad (4.21)$$

and

$$I_6 = \int_{K_4}^{\infty} F_6(K) \frac{dK}{\sqrt{K - K_4}} \quad (4.22)$$

where

$$F_5(K) = (P_i^2 + Q_i^2) \left\{ \frac{(\tau K - 1)^4 \operatorname{sgn}(\tau K - 1)}{\tau \sqrt{[(\tau K - 1)^2 + K](K_4 - K)}} \right\} \left\{ 4 \cos^2 \left[ \sqrt{b} \sqrt{(\tau K - 1)^4 - K^2} \right] \right\} \quad (4.23)$$

and

$$F_6(K) = (P_i^2 + Q_i^2) \left\{ \frac{(\tau K - 1)^4 \operatorname{sgn}(\tau K - 1)}{\tau \sqrt{[(\tau K - 1)^2 + K](K - K_3)}} \right\} \left\{ 4 \cos^2 \left[ \sqrt{b} \sqrt{(\tau K - 1)^4 - K^2} \right] \right\} \quad (4.24)$$

By changing the variables,  $x = \sqrt{K_3 - K}$  for (4.21) and  $x = \sqrt{K - K_4}$  for (4.22), (4.21) and (4.22) reduce to:

$$I_5 = 2 \int_0^{\infty} F_5(K_3 - x^2) dx \quad (4.25)$$

and

$$I_6 = 2 \int_0^{\infty} F_6(K_4 - x^2) dx \quad (4.26)$$

where we can use the Gauss-Legendre quadrature formula for each sub-integral after dividing the semi-infinite integrals into finite ones as done for  $I_2$  and  $I_4$ .

$\int_{-1}^1 F(z) dz = \sum_{i=0}^n w_i F(z_i)$	
Roots ( $z_i$ )	Weight Factors ( $w_i$ )
<i>Two-Point Formula</i>	
$n = 1$	
$\pm 0.57735 \ 02691 \ 89626$	1.00000 00000 00000
<i>Three-Point Formula</i>	
$n = 2$	
0.00000 00000 00000	0.88888 88888 88889
$\pm 0.77459 \ 66692 \ 41483$	0.55555 55555 55556
<i>Four-Point Formula</i>	
$n = 3$	
$\pm 0.33998 \ 10435 \ 84856$	0.65214 51548 62546
$\pm 0.86113 \ 63115 \ 94053$	0.34785 48451 37454
<i>Five-point Formula</i>	
$n = 4$	
0.00000 00000 00000	0.56888 88888 88889
$\pm 0.53846 \ 93101 \ 05683$	0.47862 86704 99366
$\pm 0.90617 \ 98459 \ 38664$	0.23692 68850 56189
<i>Six-Point Formula</i>	
$n = 5$	
$\pm 0.23861 \ 91860 \ 83197$	0.46791 39345 72691
$\pm 0.66120 \ 93864 \ 66265$	0.36076 15730 48139
$\pm 0.93246 \ 95142 \ 03152$	0.17132 44923 79170
<i>Ten-Point Formula</i>	
$n = 9$	
$\pm 0.14887 \ 43389 \ 81631$	0.29552 42247 14753
$\pm 0.43339 \ 53941 \ 29247$	0.26926 67193 09996
$\pm 0.67940 \ 95682 \ 99024$	0.21908 63625 15982
$\pm 0.86506 \ 33666 \ 88985$	0.14945 13491 50581
$\pm 0.97390 \ 65285 \ 17172$	0.06667 13443 08688
<i>Fifteen-Point Formula</i>	
$n = 14$	
0.00000 00000 00000	0.20257 82419 25561
$\pm 0.20119 \ 40939 \ 97435$	0.19843 14853 27111
$\pm 0.39415 \ 13470 \ 77563$	0.18616 10001 15562
$\pm 0.57097 \ 21726 \ 08539$	0.16626 92058 16994
$\pm 0.72441 \ 77313 \ 60170$	0.13957 06779 26154
$\pm 0.84820 \ 65834 \ 10427$	0.10715 92204 67172
$\pm 0.93727 \ 33924 \ 00706$	0.07036 60474 88108
$\pm 0.98799 \ 25180 \ 20485$	0.03075 32419 96117

Table 1. Roots of the Legendre Polynomials  $P_{n+1}(z)$  and the Weight Factors for the Gauss-Legendre Quadrature [1]

### 4.3 The Integration of the Hull Function $(P_i, Q_i)$

In section 3.2,  $(P_i, Q_i)$  were defined as:

$$\begin{Bmatrix} P_i \\ Q_i \end{Bmatrix} = \int_{-L}^L \left\{ \int_{-T}^0 \left( \zeta \frac{\partial h}{\partial \xi} - \xi \frac{\partial h}{\partial \zeta} \right) e^{v\zeta(\tau K-1)^2} d\zeta \right\} \begin{cases} \sin(vK\xi) \\ \cos(vK\xi) \end{cases} d\xi \quad (4.27)$$

and

$$\begin{Bmatrix} P_2 \\ Q_2 \end{Bmatrix} = \int_{-L}^L \left\{ \int_{-T}^0 \frac{\partial h}{\partial \zeta} e^{K\zeta(\tau K-1)^2} d\zeta \right\} \begin{cases} \sin(vK\xi) \\ \cos(vK\xi) \end{cases} d\xi \quad (4.28)$$

where  $i = 1$  is for pitch and  $i = 2$ , for heave. Since the integrals in the braces are functions of  $K$ ,  $\tau$  and  $\xi$ , they can be easily evaluated numerically for given values of  $K$ ,  $\tau$  and for a given section. After the sectional integration, integrations along the length of the hull are performed.

If the values of  $v$ ,  $\tau$  and  $K$  are given and if we let the inner integrals in (4.27) and (4.28) be  $f_i(\xi)$ , then:

$$\begin{Bmatrix} P_i \\ Q_i \end{Bmatrix} = \int_{-L}^L f_i(\xi) \begin{cases} \sin \alpha \xi \\ \cos \alpha \xi \end{cases} d\xi \quad \begin{array}{ll} i = 1; \text{pitch} \\ i = 2; \text{heave} \end{array} \quad (4.29)$$

where  $\alpha$  is some constant. The integral of the form (4.29) can be evaluated using the concept of the Filon-Trapezoidal quadrature [12]. The basic idea is to approximate  $f_i(\xi)$  by a linear function  $(a_i \xi + b_i)$ , say, between the intervals  $\xi_i$  and  $\xi_{i+1}$ . Then  $(P_i, Q_i)$  can be approximated:

$$\begin{Bmatrix} P_i \\ Q_i \end{Bmatrix} \doteq \sum_{i=1}^N \int_{\xi_i}^{\xi_{i+1}} (a_i \xi + b_i) \begin{cases} \sin \alpha \xi \\ \cos \alpha \xi \end{cases} d\xi \quad (4.30)$$

where  $\xi_1 = -L$  and  $\xi_{N+1} = L$ .

## V. RESULTS AND DISCUSSIONS

A computer program in Fortran IV, based on the analysis of this report, has been developed, and calculations have been performed for the sample model (Fig. 5) for several Froude numbers using the IBM 360/370 computer at the MIT Information Processing Center.

As input data, we must supply the offsets of each section of the hull. If there is a parallel middle body, we need to give only the offsets of the beginning and ending sections of the parallel middle body. The offsets of the remaining sections in the parallel middle body can be omitted. For instance, the offsets of the stations 9 and 11 are sufficient to take care of the parallel middle body in the sample model (Fig. 5).

The most time-consuming computer operations occur when evaluating the semi-infinite integrals, especially due to the highly oscillatory cosine term for twin hulls. Numerical convergence of these integrals becomes slower as the Froude number increases.

Calculations were made for Froude numbers 0.0, 0.2, and 0.4. In Figures 6 through 11, theoretical heave damping coefficients are compared with Lee's experiments [6]. In Tables 3 through 5, computer outputs of theoretical pitch damping coefficients are listed. It is to be noted in particular that the pitch damping coefficient for Froude number 0.4 at low frequencies becomes negative (Table 5). The negative damping in the present study is not easy to explain. But if it is physically realistic, it implies that the ship will be unstable in pitch at high speed. The presence of negative damping was noticed for an oscillating ellipsoid

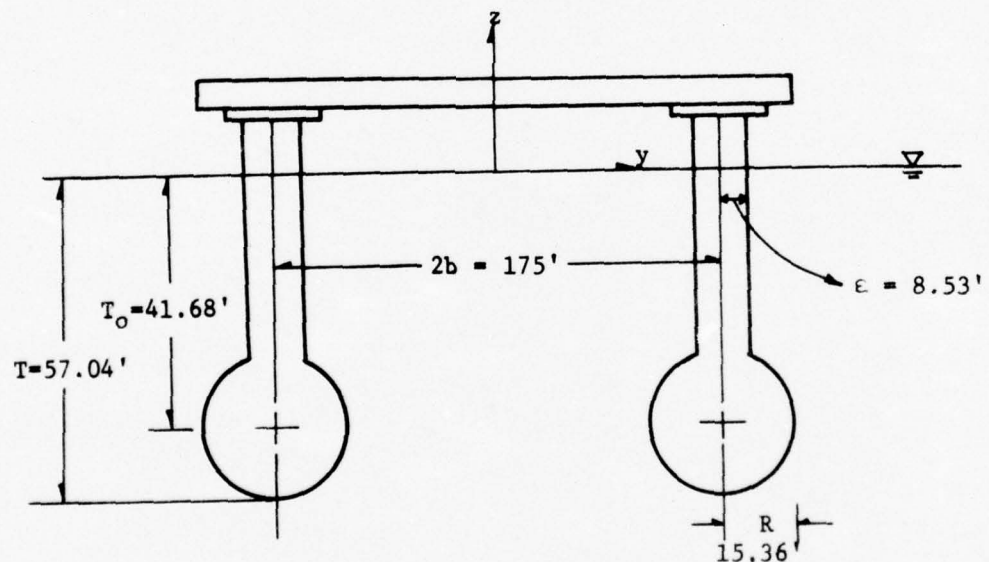
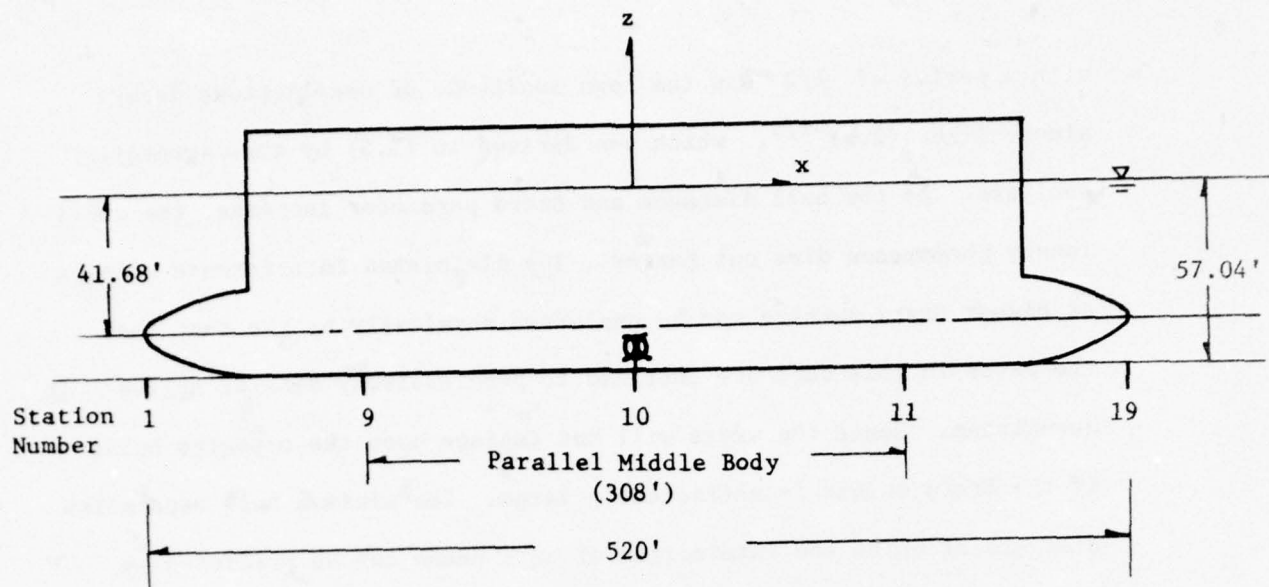
near a free surface by Newman [9] and by Gerritsma, Kerwin and Newman [5] for the Series 60 hull forms. In the present case, where the hull geometry is such that zero or minimal damping can occur at zero speed, one anticipates that negative damping may occur sooner than was observed in [5] and [9].

In both Figures and Tables, it is to be noted that when the forward speed effects are considered there are peak values of damping coefficients at critical frequencies; 1.25 at  $F_n = 0.2$  and 0.625 at  $F_n = 0.4$  for which  $\tau = 1/4$ . Although the qualitative agreement is good, the theoretical predictions are seen to be somewhat lower in the higher frequency range and higher in the lower frequency range, especially near the critical frequencies at  $\tau = 1/4$ .

In Figures 2 and 3, thin-ship and modified thin-ship results for two-dimensional cylindrical bodies are compared with Frank's [4] and Lee's [6] works. Correction factors in the modified thin-ship approach may vary depending on the hull forms and the frequencies. At high frequencies the modified thin-ship results with a correction factor of 2 give excessive damping, but in the frequency range of practical importance this modified theory agrees better with Frank's and Lee's results than does the pure thin-ship theory.

In Figures 12 through 14, damping coefficients are plotted against hull distance variations for Froude numbers 0.0, 0.05 and 0.4 at a fixed non-dimensionalized frequency 4.0. In order to investigate the Brard parameter influence on damping as well, Froude numbers are chosen such that  $\tau = 0.0, 0.2$  and 1.6 for each case. In Figure 12 it is verified that heave damping coefficients at zero forward speed oscillate

with a period of  $\lambda/2$  and the mean amplitude of oscillations decays almost like  $(2vb)^{-1/2}$ , which was derived in (3.5) by the asymptotic analysis. As the hull distance and Brard parameter increase, the oscillatory phenomenon dies out faster. The diminished interference effects at higher Brard numbers can be explained physically by the fact that the waves in this case are confined to progressively smaller angles downstream. Hence the waves will not impinge upon the opposite hulls if the Brard number is sufficiently large. The minimum hull separation distance at which the interaction effects cease can be predicted by finding the generated wave angles from Fig. 1 in [8].



Midship Section (Station 10)

Fig. 5 Dimensions of SWATH Catamaran for the Sample Program

<u>STN</u>	<u>X(I)</u>	<u>EPS(I)</u>	<u>TO(I)</u>	<u>R(I)</u>
1	-261.00	0.00	41.68	0.00
2	-250.00	0.00	41.68	5.46
3	-240.60	0.00	41.68	11.16
4	-230.00	0.00	41.68	13.38
5	-220.00	1.52	41.68	14.27
6	-209.00	3.04	41.68	15.19
7	-198.00	5.19	41.68	15.36
8	-176.00	7.85	41.68	15.36
9	-154.00	8.53	41.68	15.36
10	0.00	8.53	41.68	15.36
11	154.00	8.53	41.68	15.36
12	176.00	9.72	41.68	15.29
13	198.00	5.12	41.68	14.37
14	209.00	2.87	41.68	13.48
15	220.00	1.44	41.68	12.32
16	229.80	0.00	41.68	10.62
17	239.50	0.00	41.68	8.09
18	249.50	0.00	41.68	4.61
19	259.00	0.00	41.68	0.00

Table 2. Offset Data for the Sample Program

Froude Number = 0.0

$B_{55}$  = Pitch Damping Coefficient

$$= \frac{\text{Damping}}{\rho V L \sqrt{g} L}$$

$V$  = Displaced Volume

$\omega_e$  = Encountering Frequency =  $\omega$  at  $F_n = 0.0$

$\omega_e \sqrt{L/g}$	$B_{55}$ Single Hull	$B_{55}$ Twin Hulls
0.5	0.10851E-05	0.21689E-05
1.0	0.64874E-04	0.12846E-03
1.5	0.17057E-03	0.32428E-03
2.0	0.10922E-03	0.14321E-03
2.5	0.25516E-02	0.15228E-02
3.0	0.96172E-02	0.37951E-02
3.5	0.17570E-01	0.13984E-01
4.0	0.20316E-01	0.35164E-01
4.5	0.18057E-01	0.19299E-01
5.0	0.14401E-01	0.33401E-02
5.5	0.95581E-02	0.14782E-01
6.0	0.54997E-02	0.56590E-02
6.5	0.28302E-02	0.13068E-02

Table 3. Theoretical Results of the Pitch Damping Coefficients

Froude Number = 0.2

$B_{55}$  = Pitch Damping Coefficient

$$= \frac{\text{Damping}}{\rho V L \sqrt{g} L}$$

$V$  = Displaced Volume

$\omega_e$  = Encountering Frequency

$\omega_e \sqrt{L/g}$	$B_{55}$ <u>Single Hull</u>	$B_{55}$ <u>Twin Hulls</u>
1.00	0.78276E-02	0.39147E-02
1.25	0.18242E-01	0.23052E-01
1.50	0.91238E-02	0.58606E-02
2.00	0.80448E-02	0.57695E-02
2.50	0.93458E-02	0.70857E-02
3.00	0.10716E-01	0.13841E-01
3.50	0.11544E-01	0.14518E-01
4.00	0.11595E-01	0.71407E-02
4.50	0.10893E-01	0.12743E-01
5.00	0.97016E-02	0.13490E-01

Table 4. Theoretical Results of the Pitch Damping Coefficients

Froude Number = 0.4

$B_{55}$  = Pitch Damping Coefficient

$$= \frac{\text{Damping}}{\rho \nabla L \sqrt{gL}}$$

$\nabla$  = Displaced Volume

$\omega_e$  = Encountering Frequency

$\omega_e \sqrt{L/g}$	$B_{55}$ <u>Single Hull</u>	$B_{55}$ <u>Twin Hulls</u>
0.250	-0.81562E-02	0.66851E-03
0.500	-0.64218E-02	-0.30374E-02
0.625	-0.12086E-02	0.29785E-02
0.750	-0.24313E-02	-0.38668E-02
1.000	0.20595E-02	-0.21786E-02
1.500	0.78046E-02	0.51413E-02
2.000	0.84687E-02	0.10173E-01
2.500	0.88749E-02	0.11627E-01
3.000	0.88978E-02	0.95881E-02
3.500	0.73347E-02	0.60902E-02
4.000	0.58270E-02	0.46028E-02
4.500	0.54560E-02	0.54672E-02
5.000	0.54788E-02	0.63667E-02
5.500	0.52273E-02	0.60154E-02
6.000	0.47029E-02	0.49008E-02
6.500	0.39953E-02	0.37948E-02
7.000	0.31860E-02	0.29722E-02
7.500	0.24167E-02	0.23651E-02

Table 5. Theoretical Results of the Pitch Damping Coefficients

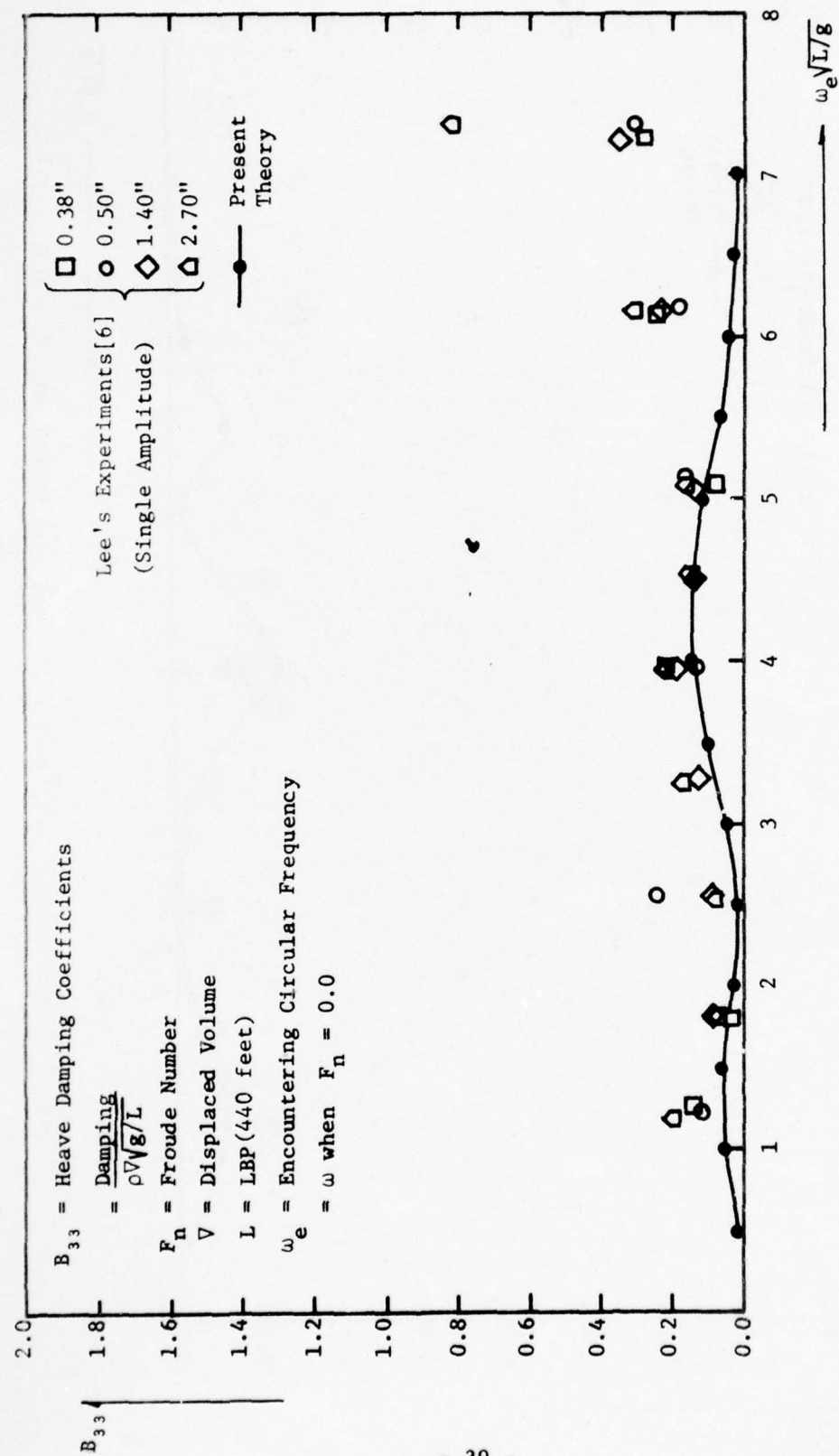


Fig. 6 Heave Damping Coefficients of Single Hull MODCAT at  $F_n = 0.0$

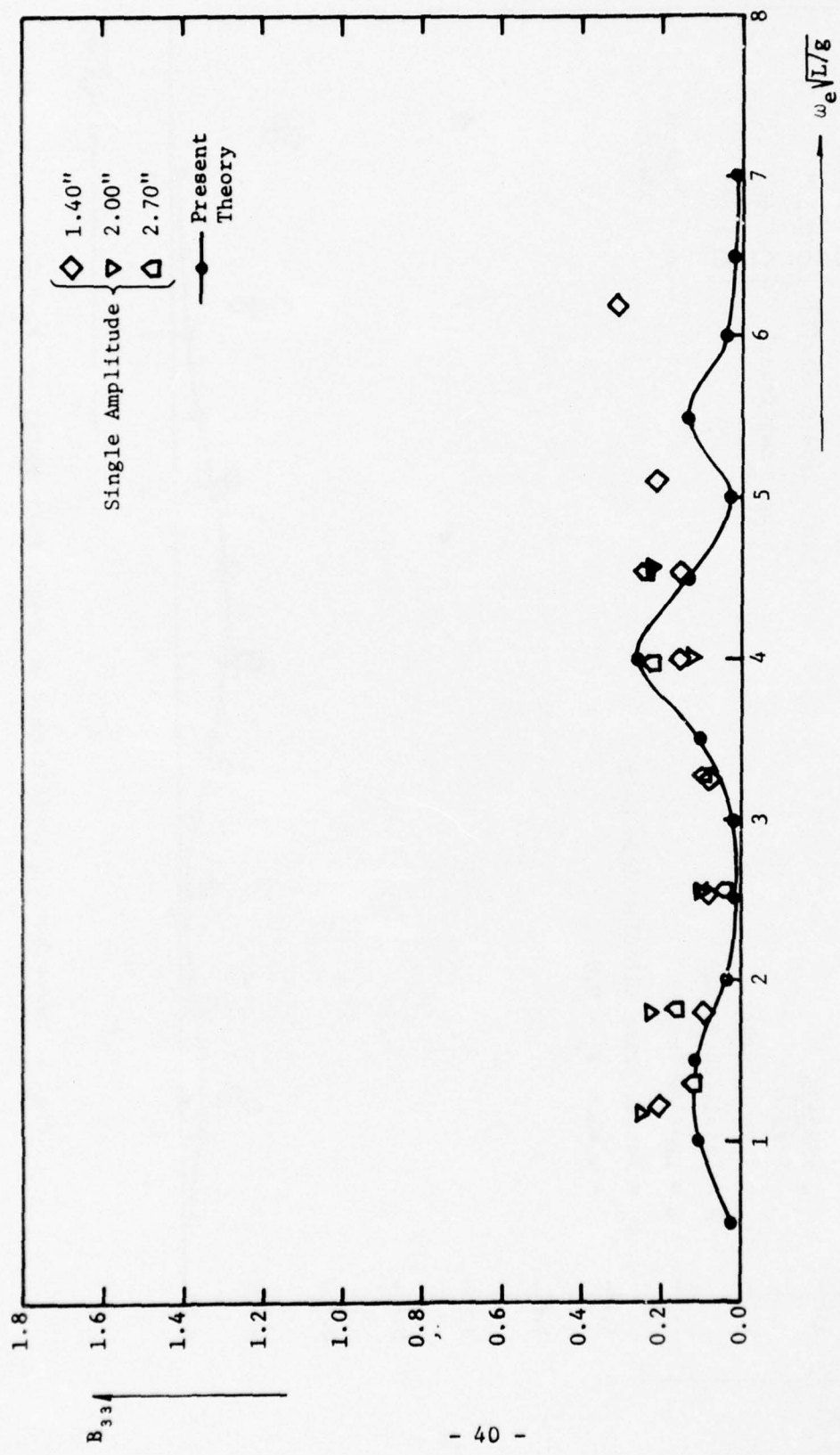


Fig. 7 Heave Damping Coefficients of Twin Hull MODCAT at  $F_n = 0.0$

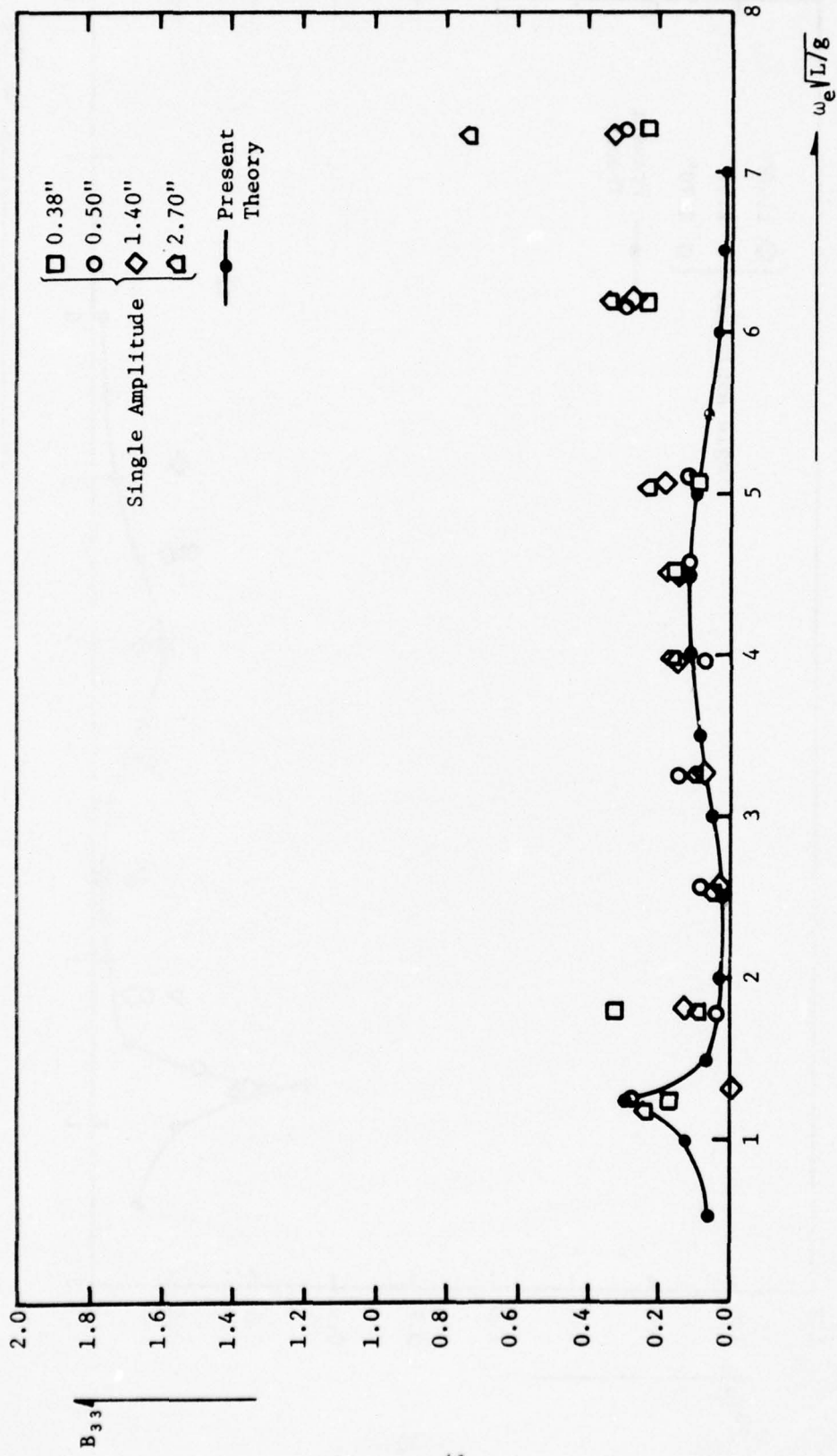


Fig. 8 Heave Damping Coefficients of Single Hull MODCAT at  $F_n = 0.20$

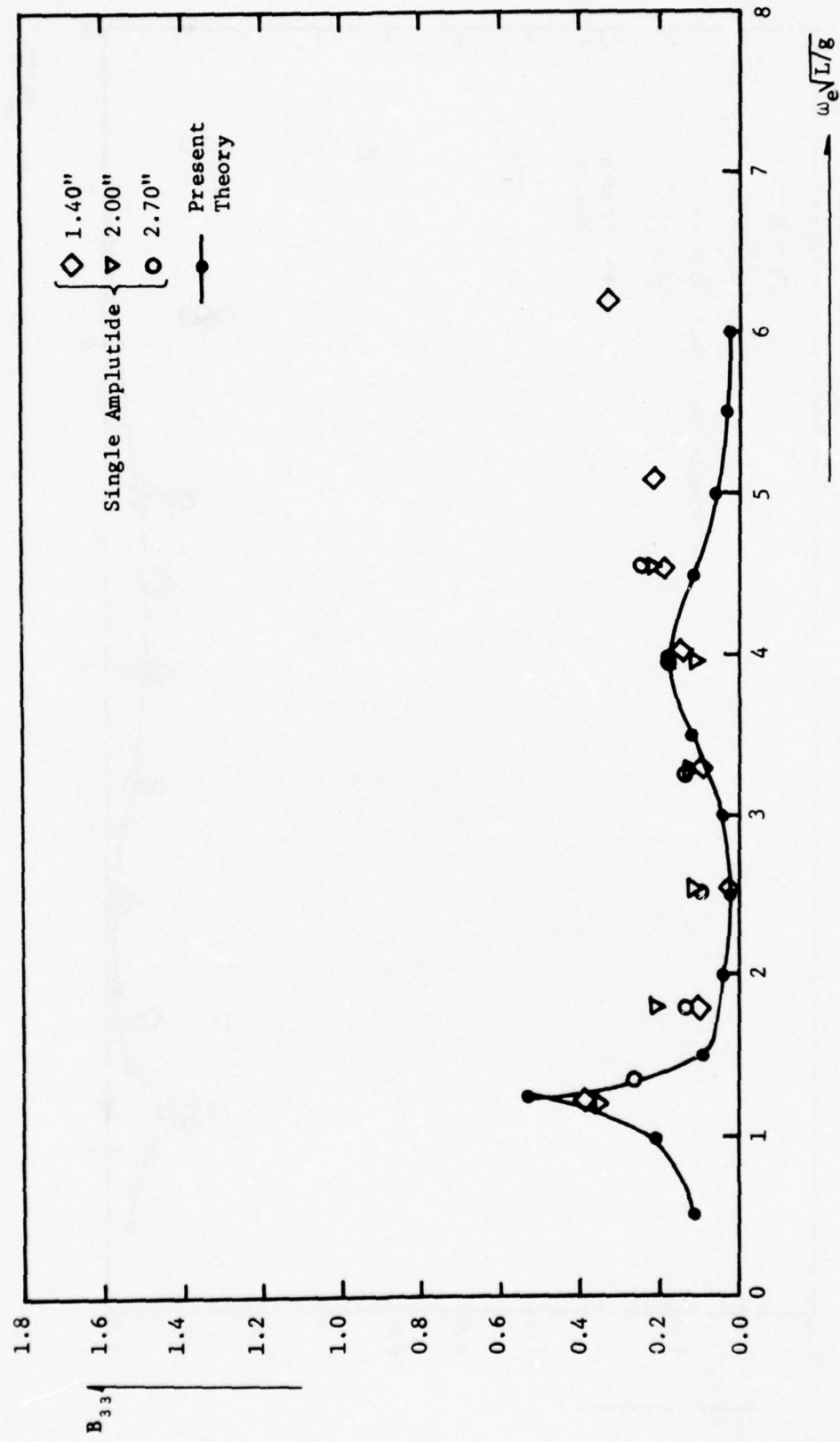


Fig. 9 Heave Damping Coefficients of Twin Hull MODCAT at  $F_n = 0.20$

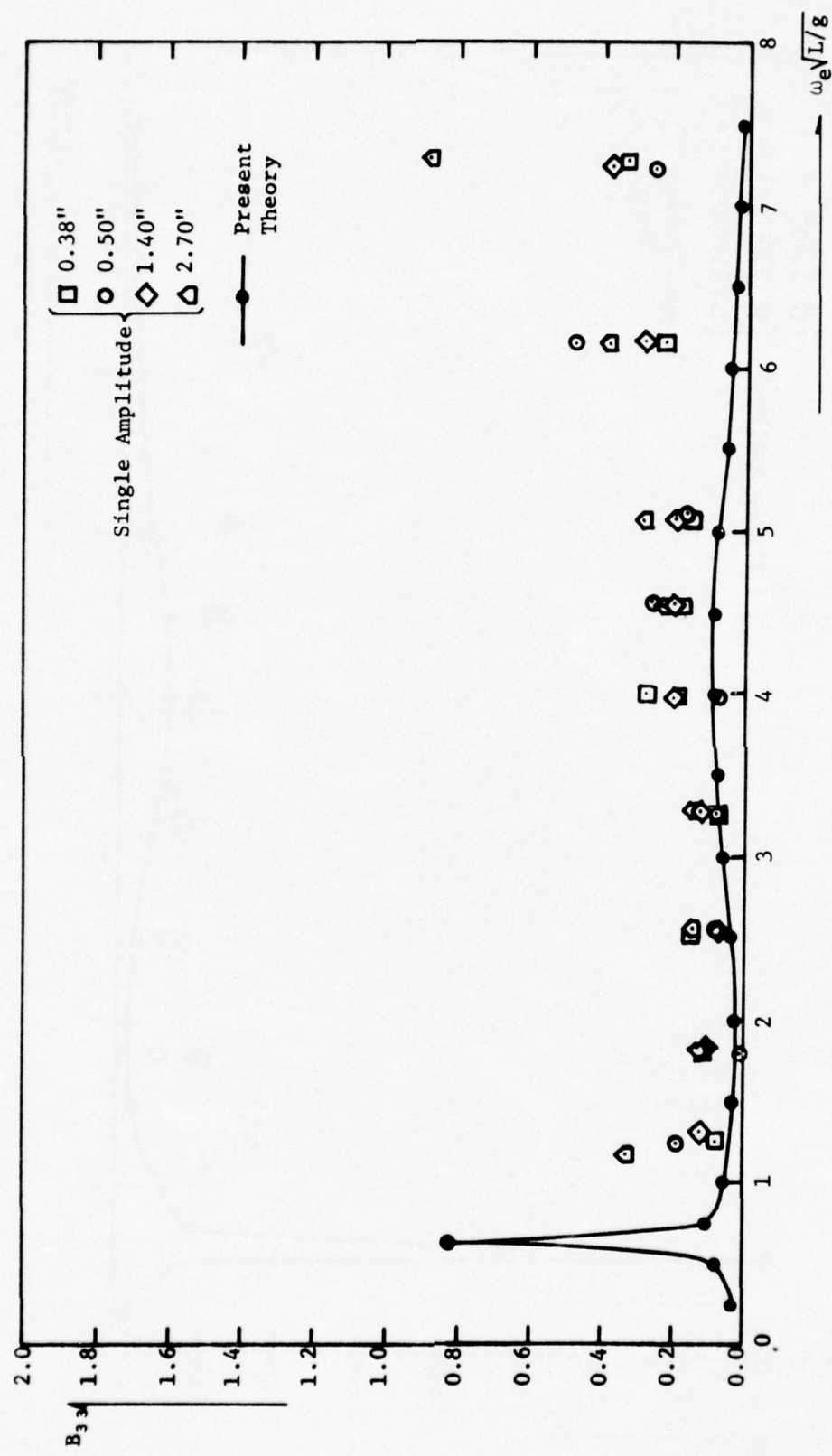


Fig. 10 Heave Damping Coefficients of Single Hull MODCAT at  $F_n = 0.40$ .

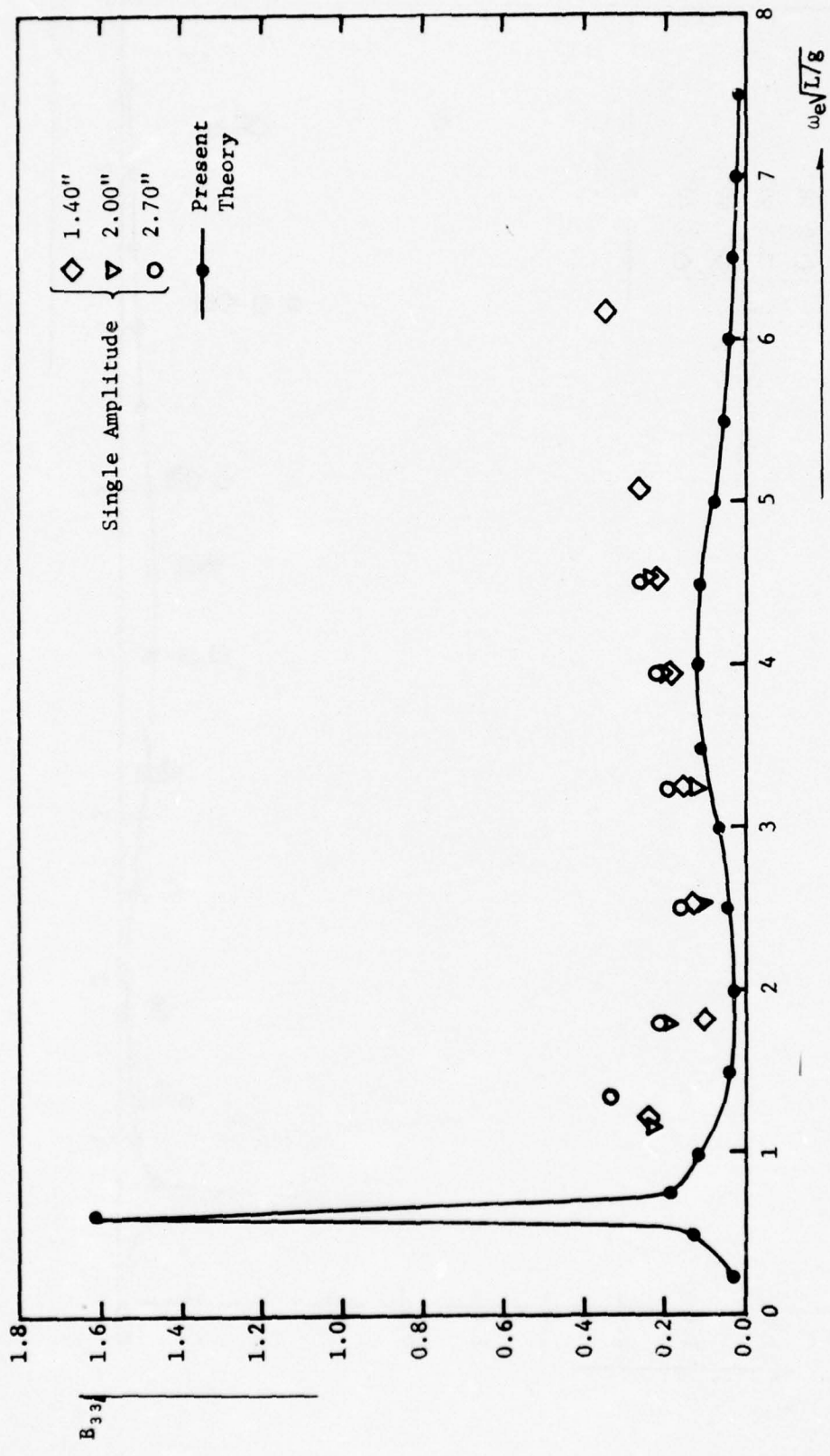


Fig. 11 Heave Damping Coefficients of Twin Hull MODCAT at  $F_n = 0.40$

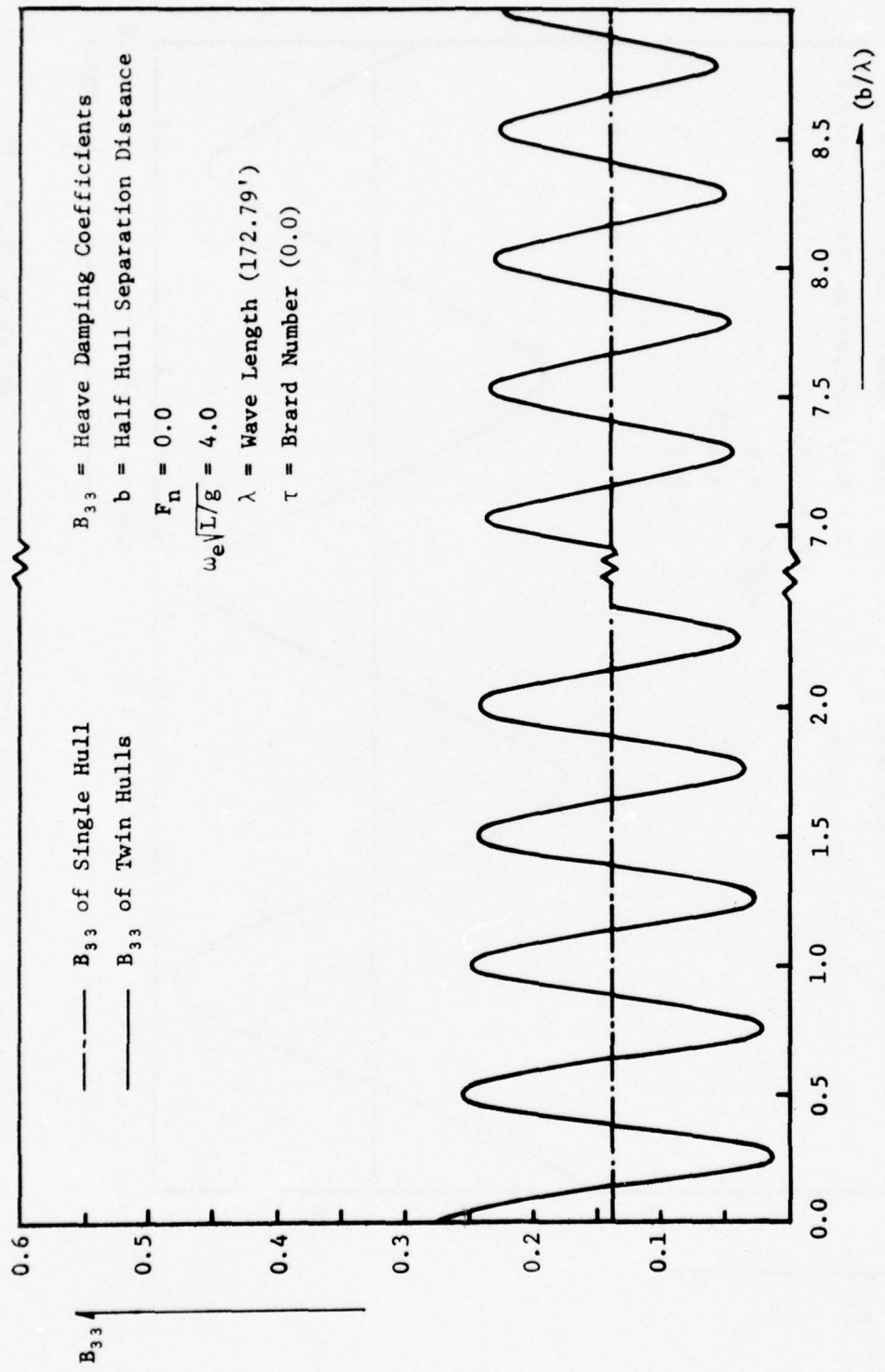


Fig. 12 The Effect of Hull Distance Variations on Damping at  $F_n = 0.0$

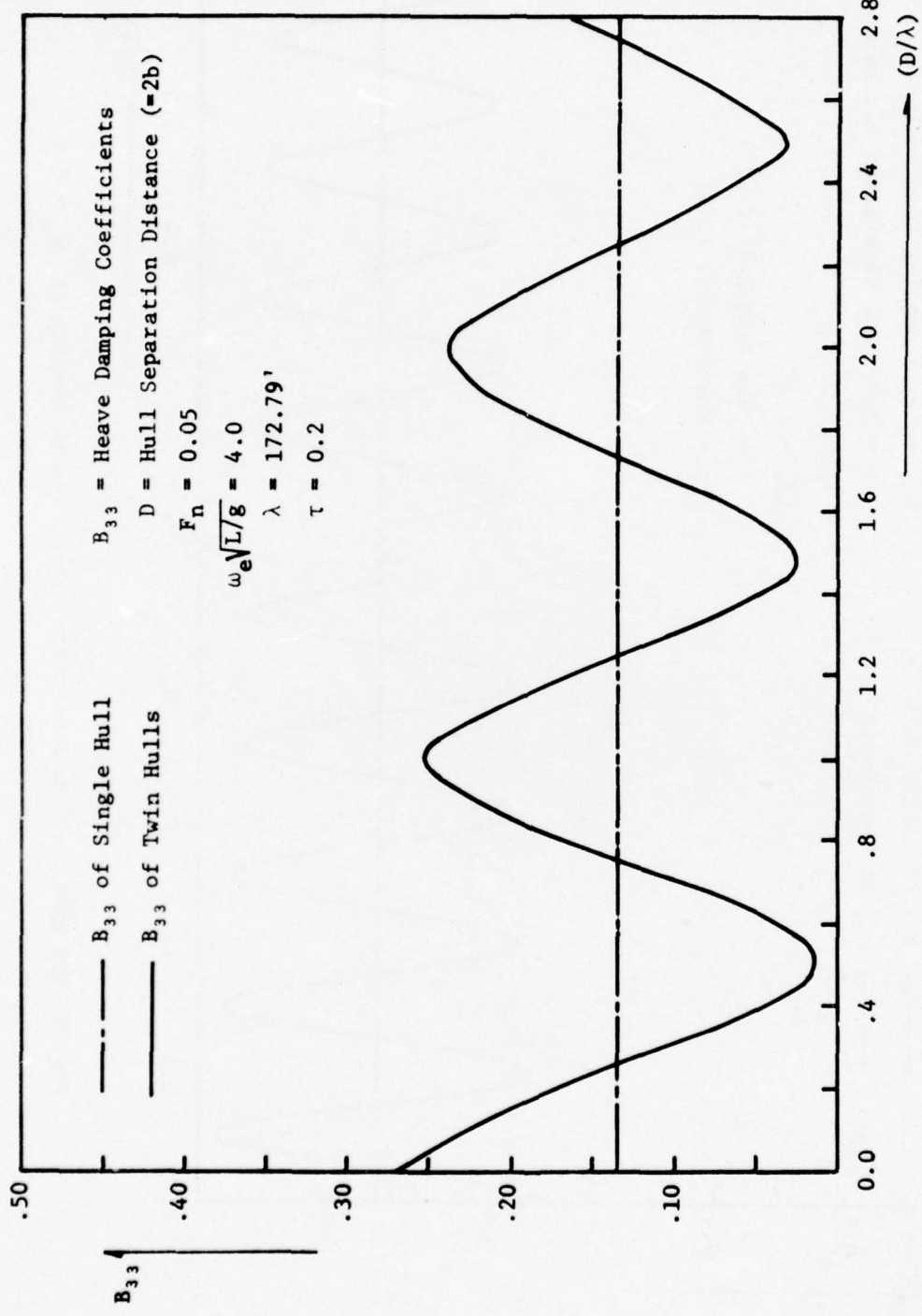


Fig. 13 The Effect of Hull Distance Variations on Damping at  $F_n = 0.05$

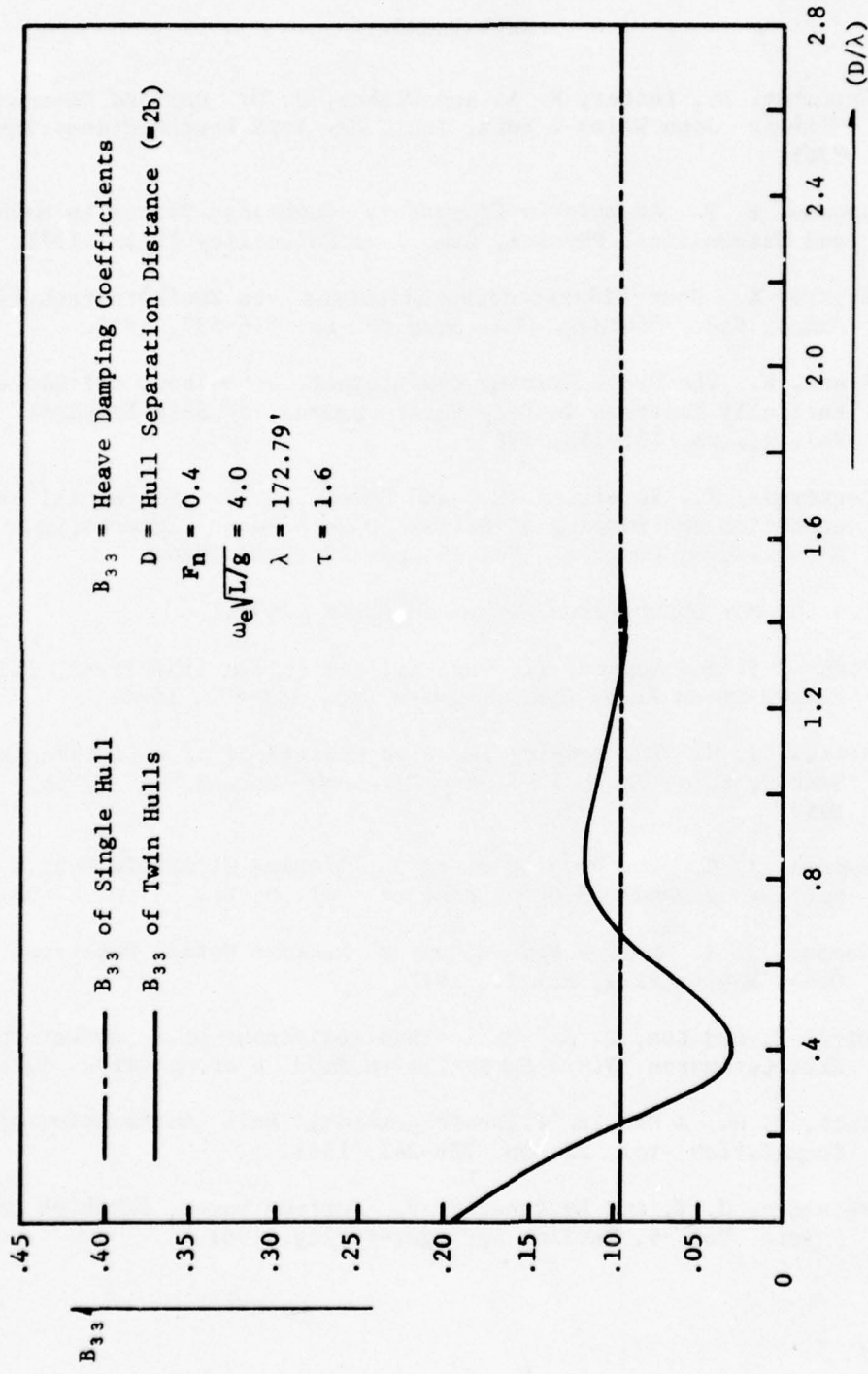


Fig. 14 The Effect of Hull Distance Variations on Damping at  $F_h = 0.4$

#### REFERENCES

1. Carnahan, B., Luther, H. A. and Wilkes, J. O. *Applied Numerical Methods* John Wiley & Sons, Inc., New York.London.Sydney.Toronto, 1969.
2. Copson, E. T. *Asymptotic Expansions* Cambridge Tracts in Mathematics and Mathematical Physics, Cambridge University Press, 1971.
3. Eggers, K. Über Widerstandsverhältnisse von Zweikörperschiffen *Jahrb. Schiffbautech. Ges. Band 49* pp. 516-537, 1955.
4. Frank, W. The Heave Damping Coefficients of Bulbous Cylinders, Partially Immersed in Deep Water *Journal of Ship Research* Vol. 11, pp. 151-153, 1967.
5. Gerritsma, J., Kerwin, J. E., and Newman, J. N. Polynomial Representation and Damping of Series 60 Hull Forms *International Shipbuilding Progress* Vol. 9, pp. 295-304, 1964.
6. Lee, C. M. *Unpublished Report in NSRDC* 1974.
7. Motora, S. and Koyama, T. Wave Excitationless Ship Forms *Sixth Symposium on Naval Hydrodynamics* pp. 383-404, 1966.
8. Newman, J. N. The Damping and Wave Resistance of a Pitching and Heaving Ship *Journal of Ship Research* Vol. 3, No. 1, pp. 1-19, 1959.
9. Newman, J. N. The Damping of an Oscillating Ellipsoid Near a Free Surface *Journal of Ship Research* Vol. 5, No. 3, pp. 44-58, 1961.
10. Newman, J. N. *Marine Hydrodynamics* Lecture Notes, Department of Ocean Engineering, M.I.T., 1971.
11. Pien, P. and Lee, C. M. Motion and Resistance of a Low-Waterplane-Area Catamaran *Ninth Symposium on Naval Hydrodynamics* 1972.
12. Tuck, E. O. A Simple 'Filon-Trapezoidal' Rule *Mathematics of Computation* Vol. 21, pp. 239-241, 1967.
13. Wehausen, J. V. and Laitone, E. V. Surface Waves *Handbuch der Physik* Vol. 9, Berlin: Springer-Verlag, 1961.

## APPENDIX A

### INPUT AND OUTPUT

#### INPUT DATA

##### DATA CARD 1 - FORMAT (I10, 2F10.2)

NST = The number of offset stations of the hull.

AL = Length at the waterline.

B = Half hull separation distance.

##### DATA CARDS 2 - FORMAT (4F10.4)

Data cards 2 consist of NST number of cards, on each of which the values of X, EPS, TO, R should be punched according to the above format.

X(I) = An array of the x-coordinates of the stations.

EPS(I) = An array of the half-beam at the waterline.

TO(I) = An array of the distance  $T_o$ . (See Fig. 5)

R(I) = An array of the radius of each section.

##### DATA CARD 3 - FORMAT (2I10)

NFR = The number of Froude numbers to be tested.

NOM = The number of non-dimensionalized circular frequencies to be tested.

##### DATA CARD(S) 4 - FORMAT (8F10.4)

FR(I) = An array of NFR number of Froude numbers.

OM(I) = An array of NOM number of the non-dimensionalized circular frequencies.

Besides the input data cards, we must supply the roots of the Legendre polynomials and the weight factors for the Gauss-Legendre quadrature in order to evaluate the semi-infinite integrals,  $I_2$ ,  $I_4$ ,  $I_5$  and  $I_6$ . In the sample program, the ten-point Gauss-Legendre quadrature formula is used.

OUTPUT

Major outputs are pitch and heave damping coefficients of a single and twin hulls. However, we can get various intermediate results for checking purposes.

DP1(I) = An array of the pitch damping coefficients of a single hull.

DP2(I) = An array of the pitch damping coefficients of twin hulls.

DH1(I) = An array of the heave damping coefficients of a single hull.

DH2(I) = An array of the heave damping coefficients of twin hulls.

## APPENDIX B

### PROGRAM DESCRIPTIONS

#### Main Program

The main program handles input and output, calculates various parameters and performs six integrals in (3.8), (3.9), and (3.10) calling subroutines PIQI and ROOT. Gauss-Chebyshev quadrature formula is used for  $I_1$  and  $I_3$ . For the rest of the integrals, the subroutine ROOT is called in order to determine the size A for the sub-integrals. (See Section 4.2.)

#### Subroutine PIQI

This subroutine integrates the hull function  $(P_i, Q_i)$  in (4.27) and (4.28) for a given section first and then integrates along the length of the hull. It gives the values of  $\{P_i^2(K) + Q_i^2(K)\}$  for given values of  $K$ ,  $v$ , and  $\tau$ .

#### Subroutine ZETIN

For given values of  $v$ ,  $\tau$ ,  $K$  and for a given section (i.e.,  $\epsilon$ ,  $T_0$ ,  $r$ ), this subroutine evaluates the integral,

$$\gamma v(\tau K - 1)^2 \int_{-T}^{-H} h(\xi, \zeta) e^{v\zeta(\tau K - 1)^2} d\zeta \quad (A.1)$$

by using Simpson's rule and returns the resulting value through the variable Z. The  $\gamma$  in (A.1) is the correction factor for the cylindrical part explained in Section 2.3. This subroutine is used for both  $(P_1, Q_1)$  and  $(P_2, Q_2)$ .

### Subroutine ZETINS

This subroutine evaluates the integral:

$$\int_{-T}^{-H} h(\xi, \zeta) \zeta e^{v\zeta(\tau K-1)^2} d\zeta \quad (A.2)$$

by using Simpson's rule, which is similar to that in ZETIN. The resulting values are returned through the variable ZS which is used only for  $(P_1, Q_1)$ .

### Subroutine ROOT

This subroutine evaluates the zeros of  $\cos(2vb\sqrt{(\tau K-1)^4 - K^2}) = 0$ , from which we get a polynomial equation:

$$(\tau K-1)^4 - K^2 = \left(\frac{n\pi}{2vb}\right)^2, \quad (n = 1, 2, 3, \dots) \quad (A.3)$$

The roots of this polynomial are found by calling the IBM Scientific Subroutine Package POLRT. The subroutine ROOT is used in evaluating the semi-infinite integrals.

### Function SS

This function calculates the submerged area of a given section. It is used in evaluating the displacement of the hull in the main program.

### Function F

This function evaluates the integrand in (A.1) for the purpose of Simpson's rule.

### Function S

This function evaluates the integrand in (A.2) for the purpose of Simpson's rule.

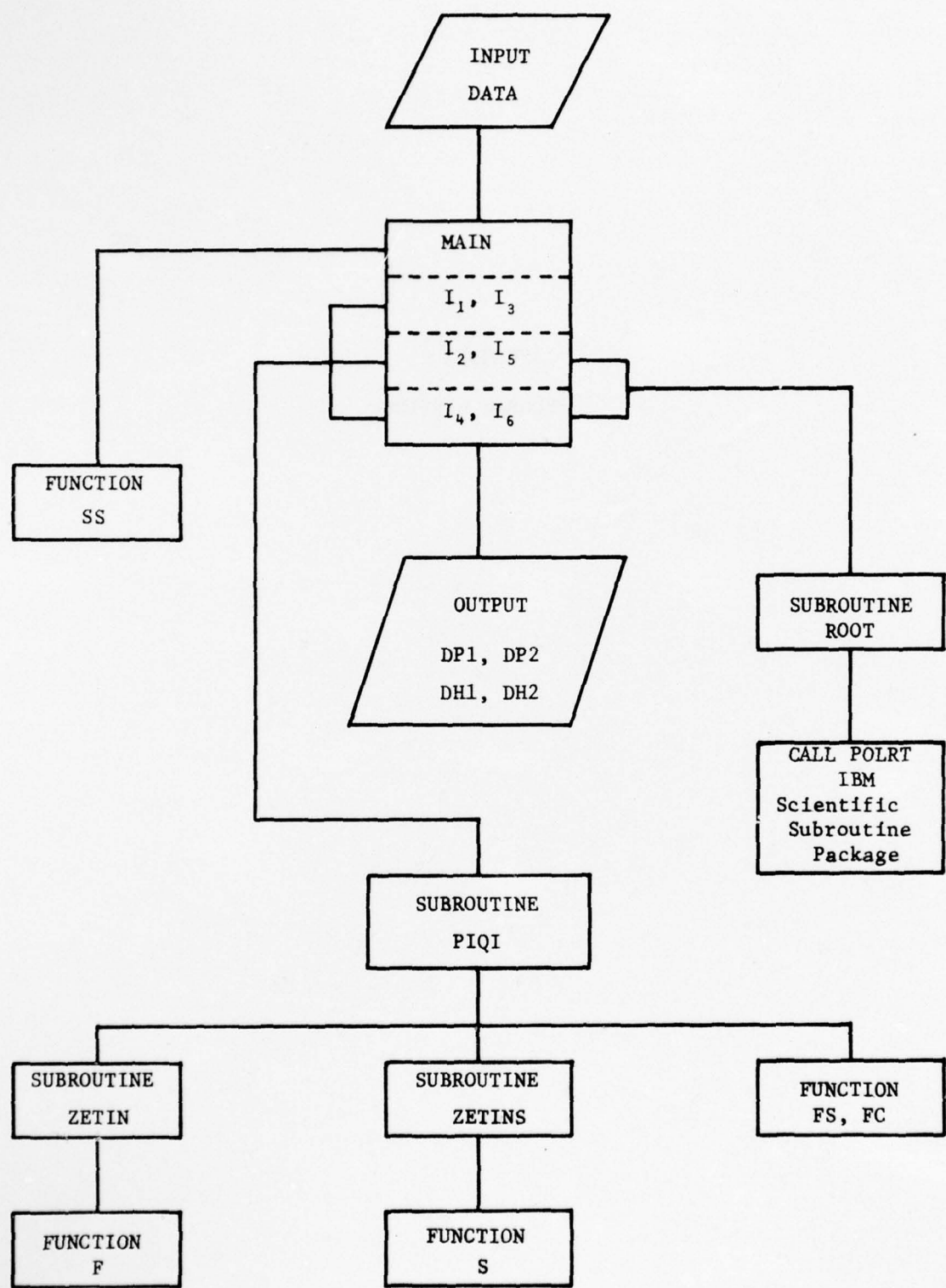


Fig. 15 Flow Chart

**APPENDIX C**  
**PROGRAM LISTING**

```

C.....THIS PROGRAM COMPUTES TEP PITCH AND HEAVE DAMPING COEFFICIENTS
C.....OF A SINGLE AND TWIN HULLS SWATH CONFIGURATIONS INCLUDING FORWARD
C.....SEED EFFECTS, BASED ON NEWMAN'S THIN-SHIP THEORY.
      DIMENSION TAU(10,30),BNU(10,30)
      DIMENSION DH1(30),DH2(30),DP1(30),DP2(30)
      DIMENSION Z(10),WEIT(10)
      DIMENSION FR(10),OM(30)

C     COMMON /GEOM/ NST,NST,XES(40),R(40),TO(40),X(40)
C     COMMON /ONE/ ROOTR(4),RCOTT(4)

C     DATA L/5/, M/6/

C.....ROOTS OF THE 10-POINT(N=9) LEGENDRE POLYNOMIALS
      Z(1)=.148874
      Z(2)=.433395
      Z(3)=.679409
      Z(4)=.865063
      Z(5)=.973906

C     C.....WEIGHT FACTORS FOR THE 10-POINT GAUSS-LEGENDRE QUADRATURE
      WEIT(1)=.295524
      WEIT(2)=.269256
      WEIT(3)=.219046
      WEIT(4)=.149451
      WEIT(5)=.066671

C     DO 100 I=1,5
      J=I+5
      Z(J)=-Z(I)
      WEIT(J)=WEIT(I)
  100 CONTINUE

C     INPUT DATA
      READ (L,10) NST,AL,R
      WRITE(M,11) NST,AL,R

C     READ (L,12) (X(T),T=0,T), (X(T),T=1,T)
      READ (L,13) (X(T),T=0,T), (X(T),T=1,T)
      READ (L,14) NED,NOM
      WRITE(M,15) NED,NOM

C     READ (L,16) (PR(T),T=1,NED)
      WRITE(M,17) (PR(T),T=1,NED)

C     READ (L,18) (OM(T),T=1,NOM)
      WRITE(M,19) (OM(T),T=1,NOM)

C     10 FORMAT (T10.2E12.2)
      11 FORMAT (3X,'DATA:  WSPDC MODEL #ODCAT 5226'//,
     1           'SY, NO. OF STATIONS =',T4.5Y,
     2           'LENGTH AT THE WL =',F7.2,' (FEET)'//,
     3           'SY, WSLP HULL SPACING =',F7.2,' (FEET)'///)
      12 FORMAT (4E10.4)
      13 FORMAT (5Y,'S',N1.7Y,'X(T)',7Y,'T0S1',7Y,'T0',7X,
     1           '1'/(7,3X,4E10.3))
      14 FORMAT (2T10)
      15 FORMAT (//5Y,'NO. OF FREQUENCIES TO BE TESTED =',T3/
     1           'SY, NO. OF NON-DIM. CIRCULAR FREQ. =',T3//)
      16 FORMAT (2E10.4)
      17 FORMAT (2E10.4)
      18 FORMAT (4E10.4)
      19 FORMAT (4E10.4)

C     NST=NST-1
      ET=3.141592
      G=32.17
      NT=100
      NC1=50
      NC2=10

```

Copy available to DDC does not  
permit fully legible reproduction

```

MAIN0001
MAIN0002
MAIN0003
MAIN0004
MAIN0005
MAIN0006
MAIN0007
MAIN0008
MAIN0009
MAIN0010
MAIN0011
MAIN0012
MAIN0013
MAIN0014
MAIN0015
MAIN0016
MAIN0017
MAIN0018
MAIN0019
MAIN0020
MAIN0021
MAIN0022
MAIN0023
MAIN0024
MAIN0025
MAIN0026
MAIN0027
MAIN0028
MAIN0029
MAIN0030
MAIN0031
MAIN0032
MAIN0033
MAIN0034
MAIN0035
MAIN0036
MAIN0037
MAIN0038
MAIN0039
MAIN0040
MAIN0041
MAIN0042
MAIN0043
MAIN0044
MAIN0045
MAIN0046
MAIN0047
MAIN0048
MAIN0049
MAIN0050
MAIN0051
MAIN0052
MAIN0053
MAIN0054
MAIN0055
MAIN0056
MAIN0057
MAIN0058
MAIN0059
MAIN0060
MAIN0061
MAIN0062
MAIN0063
MAIN0064
MAIN0065
MAIN0066
MAIN0067
MAIN0068
MAIN0069
MAIN0070
MAIN0071
MAIN0072

```

```

WT1=PT/FICAT(MQ1)
WT2=PT/FICAT(MQ2)

C *****
C *   CALCULATION OF THE DEMI-HULL DISPLACEMENT   *
C *   IN CUBIC FEET FROM THE GIVEN DATA           *
C *****
C DISP=0.
DO 150 T=1,NST
J=T+1
EPS1=PPS(T)
EPS2=PPS(J)
R1=R(I)
R2=R(J)
TC1=TO(I)
TC2=TO(J)
X1=X(I)
X2=X(J)
DELY=X2-X1
DELV=SS(PPS1,TO1,R1)+SS(PPS2,TO2,R2)
150 DISP=DISP+DELV*DELY/2.
      WRITE(*,20) DISP
20 FORMAT (//5X,'DISPLACEMENT =',F10.2,'(CUBIC FEET)'//)

C.....NON-DIMENSIONALIZING FACTORS FOR PITCH & HEAVE(SINGLE HULL)
FNON=DISP*AL*SQRT(G*AL)
HNON=DISP*SQRT(G/AL)

C DO 270 I=1,NPP
V=SQRT(G*AL)*PR(I)
VN0T=V/1.689
      WRITE(*,21) PR(T),V,VN0T
21 FORMAT (//3X,'FROUDE NO=',F5.2,4X,'V (FT/S)=',F8.3,
1          '        4X,'V (KNOT)=',F8.3//)

C DO 250 J=1,40M
CMFG1=C*(J)
CMFG2=CMFG1*A2*G/AL
X1=1.07*(G*AL)
T1=1.07/VN0T
Y1=M0=2.*PR*T/(G*AL)
TTAU=VN0T*V/G
ANU=OMSG/G

C      WRITE(*,22) CMFGA,BTAU,ANU,MN,T,XLAMDA
22 FORMAT (3Y,'CMFGA,BTAU,ANU,MN,T,XLAMDA',
1          '      3X,'CMFGA(BAD/SEC.)=',F6.3,4X,'T(SRC)=',F6.3,
2          '      4X,'XLAMDA(PR)=',F8.2//)

C      TAU(T,J)=TTAU
      RNU(T,J)=ANU

C      PI1=0.
      PI2=0.
      HI1=0.
      HI2=0.

C      IF (BTAU.EQ.0.) TTAU=1
      IF (BTAU.GT.0..AND.BTAU.LE.0.25) TTAU=2
      IF (BTAU.GT.0.25) TTAU=3
      GO TO (300,350,350), TTAU

C *****
C *   ZERO FORWARD SPEED CASE (TAU=0.)           *
C *   USING 501-POINT GAUSS-CHEBYSHEV QUADRATURE *
C *****
C 300 CONTINUE
      DO 410 J1=1,401
      YKT=CDK(P10)^(2*(J1-1))*FT/EL07^(2*M01)
      Z1=T.-YKT**2

```

```

IF (Z1.LT.0.) Z1=0.
ARG=2.*ANU*P*SQRT(Z1)                                MAIN0145
C
CALL PIQ1(XKI,ANU,PTAU,FPO,HPO)                      MAIN0146
C
C.....INTERMEDIATE RESULTS CAN BE PRINTED IF DESIRED   MAIN0147
C
WRITE(M,23) XKI,ARG,PPQ,HPO                           MAIN0148
C 23 FORMAT (2F10.4,3Y,2E16.5)                         MAIN0149
C
EPQ=-PPQ                                              MAIN0150
HPQ=-PPQ                                              MAIN0151
C
PI1=PI1+PPQ                                           MAIN0152
PI2=PI2+FPQ*2.* (COS(ARG)+1.)                         MAIN0153
HI1=HI1+HPQ                                           MAIN0154
HI2=HI2+HPQ*2.* (COS(ARG)+1.)                         MAIN0155
400 CONTINUE                                         MAIN0156
C
DP1(J)=((PI1*WT1)*(-2.*RN*ANU/PI))/PNON            MAIN0157
DH1(J)=((HI1*WT1)*(-2.*RN*INU/PI))/RN0N             MAIN0158
DP2(J)=((PI2*WT1)*(-RN*ANU/PI))/PNON                MAIN0159
DH2(J)=((HI2*WT1)*(-RN*INU/PI))/RN0N                MAIN0160
GO TO 410                                            MAIN0161
C
350 CONTINUE                                         MAIN0162
C
C.....RK1,RK2,RK3,RK4: ROOTS OF (TAU*K-1.)**4-K**2=0.  MAIN0163
RK1=0.                                                 MAIN0164
RK2=0.                                                 MAIN0165
RK3=0.                                                 MAIN0166
RK4=0.                                                 MAIN0167
C
TA1=SQRT(1.-4.*PTAU)                                 MAIN0168
TA2=SQRT(1.+4.*PTAU)                                 MAIN0169
C
TE1=2.*PTAU-1.                                       MAIN0170
TR2=2.*PTAU+1.                                       MAIN0171
TAE=2.*PTAU**2                                       MAIN0172
C
RK3=(TE2-TA2)/TAB                                    MAIN0173
RK4=(TE2+TA2)/TAB                                    MAIN0174
C
IF (TTAU.F0.3) GO TO 500                            MAIN0175
C
TA1=SQRT(1.-4.*PTAU)                                 MAIN0176
RK1=(TE1-TA1)/TAB                                    MAIN0177
RK2=(TE1+TA1)/TAB                                    MAIN0178
500 CONTINUE                                         MAIN0179
C
WRITE (M,27) RK1,RK2,RK3,RK4                         MAIN0180
27 FORMAT (/5X,'K1=',F13.6,'K2=',E13.6,
           1        '4X,'K3=',E13.6,4X,'K4=',E13.6/)    MAIN0181
C
P1T2=0.                                               MAIN0182
E2T2=0.                                               MAIN0183
H1T2=0.                                               MAIN0184
H2T2=0.                                               MAIN0185
C
IF (TTAU.F0.3) GO TO 550                            MAIN0186
C
C*****                                                 MAIN0187
C * OCTAU<0.25 : FINITE INTEGRAL FROM K2 TO K3      *
C * USING MC2-POINT GAUSS-CHEBYSHEV QUADRATURE     *
C *****                                                 MAIN0188
C
A1=(RK3-RK2)/2.                                     MAIN0189
B1=(RK3+RK2)/2.                                     MAIN0190
C
DC 600 J2=1,M02                                     MAIN0191
XKI=COS(FLOAT(2*J2-1)*EI/FLOAT(2*M02))           MAIN0192
AKI=A1*XKI+B1                                      MAIN0193

```

```

C
Z1=BTAU**2*SQRT((RK4-AKI)*(AKI-RK1))          MAIN0217
Z2=(BTAU*AKI-1.)*4                            MAIN0218
Z3=Z2-AKI**2                                     MAIN0219
IF (Z3.LT.0.) Z3=0.                             MAIN0220
Z4=COS(2.*ANU*B*SQRT(Z3))                      MAIN0221
C
SGN=1.
SGNX=BTAU*AKI-1.
IF (SGNX.LT.0.) SGN=-1.
C
Z21=Z2*SGN/Z1                                     MAIN0222
Z22=Z21*(2.*Z4+2.)
C
CALL PIQI (AKI,ANU,BTAU,PPC,HPQ)                MAIN0223
C
F1=F11+PPQ*Z21                                     MAIN0224
F2=F12+PPQ*Z22                                     MAIN0225
H11=H11+HQ*Z21                                     MAIN0226
H12=H12+HQ*Z22                                     MAIN0227
MAIN0228
MAIN0229
MAIN0230
MAIN0231
MAIN0232
MAIN0233
MAIN0234
MAIN0235
MAIN0236
MAIN0237
MAIN0238
MAIN0239
MAIN0240
MAIN0241
MAIN0242
MAIN0243
MAIN0244
MAIN0245
MAIN0246
MAIN0247
MAIN0248
MAIN0249
MAIN0250
MAIN0251
MAIN0252
MAIN0253
MAIN0254
MAIN0255
MAIN0256
MAIN0257
MAIN0258
MAIN0259
MAIN0260
MAIN0261
MAIN0262
MAIN0263
MAIN0264
MAIN0265
MAIN0266
MAIN0267
MAIN0268
MAIN0269
MAIN0270
MAIN0271
MAIN0272
MAIN0273
MAIN0274
MAIN0275
MAIN0276
MAIN0277
MAIN0278
MAIN0279
MAIN0280
MAIN0281
MAIN0282
MAIN0283
MAIN0284
MAIN0285
MAIN0286
MAIN0287
MAIN0288
C.....INTERMEDIATE RESULTS CAN BE PRINTED IF DESIRED
C
WRITE (*,30) ITER
C 30 FORMAT (8X,'ITER=',I3/)
C
WRITE (*,31) (ROOTR(I1),I1=1,4), (RCOTT(I1),I1=1,4)
C 31 FORMAT (8X,'R1=',E13.6,5X,'R2=',E13.6,5X,'R3=',E13.6,5X,'R4=',E13.6,5X)
C 1   E13.6/E8X,'I1=',E13.6,5X,'I2=',E13.6,5X,'I3=',E13.6,5X,'I4=',E13.6,5X)
C 2   E13.6/)
C
WRITE (*,32) AA,PR,CXX
C 32 FFORMAT (8X,'AA=',E13.6,4X,'PR=',E13.6,4X,'CXX=',E13.6/)
C
P11=0.
P12=0.
H11=0.
H12=0.
C
C.....10-POINT GAUSS-LEGENDRE QUADRATURE FOR A GIVEN INTERVAL
DO 730 J3=1,10
XXIPR=(XTT*2*(J3)+XTT*PE)/2.
WI=WEIT(J3)

```

**COPY AVAILABLE TO DDC DOES NOT  
PERMIT FULLY LEGIBLE PRODUCTION**

```

AKI=RK1-XKBAR**2          MAIN0289
IF (ITAU.EQ.3) AKI=RK3-XKBAR**2      MAIN0290
IP (ITAU.EQ.3) GO TO 71C      MAIN0291
Z1=ETAU**2*SQRT((RK4-AKI)*(RK3-AKI)*(RK2-AKI))      MAIN0292
GO TO 72C      MAIN0293
710 Z1=ETAU*SQRT(((ETAU*AKI-1.)**2+AKI)*(RK4-AKI))      MAIN0294
720 Z2=(ETAU*AKI-1.)**4      MAIN0295
C      MAIN0296
SGN=1.      MAIN0297
SGNX=ETAU*AKI-1.      MAIN0298
IF (SGNX.LT.0.) SGN=-1.      MAIN0299
C      MAIN0300
Z3=Z2-AKI**2      MAIN0301
C      MAIN0302
Z3 SHOULD NOT BE NEGATIVE VALUE.      MAIN0303
C      MAIN0304
HOWEVER, NUMERICAL ERROR MAY GIVE VERY SMALL -- VALUE.      MAIN0305
IF (Z3.LT.0.) Z3=0.      MAIN0306
Z4=COS(2.*ANU*B*SQRT(Z3))      MAIN0307
ZZ1=Z2*SGN/Z1      MAIN0308
ZZ2=ZZ1*(2.*Z4+2.)      MAIN0309
C      MAIN0310
CALL PIQ1 (AKI,ANU,ETAU,PPQ,HPC)      MAIN0311
C      MAIN0312
PI1=PI1+XIN*WI*PPQ*ZZ1      MAIN0313
PI2=PI2+XIN*WI*PPQ*ZZ2      MAIN0314
HI1=HI1+XIN*WI*HPQ*ZZ1      MAIN0315
HI2=HI2+XIN*WI*HPQ*ZZ2      MAIN0316
700 CCNTINUE      MAIN0317
C      MAIN0318
SUMP1=SUMP1+PI1      MAIN0319
SUMP2=SUMP2+PI2      MAIN0320
SUMH1=SUMH1+HI1      MAIN0321
SUMH2=SUMH2+HI2      MAIN0322
C      MAIN0323
EROPP=AES(PI1/SUMP1)      MAIN0324
ERORH=AES(HI1/SUMH1)      MAIN0325
C      MAIN0326
WRITE (*,33) PI1,SUMP1,EROPP,PI2,SUMP2      MAIN0327
.....INTERMEDIATE RESULTS CAN BE PRINTED IF DESIRED
33 FORMAT (8X,'PI1=',E13.6,4X,'SUMP1=',E13.6,4X,'EROPP=',E10.3,
C      1        4X,'PI2=',E13.6,4X,'SUMP2=',E13.6)
C      MAIN0328
WRITE (*,34) HI1,SUMP1,ERORH,HI2,SUMH2      MAIN0329
C      MAIN0330
34 FORMAT (8X,'HI1=',E13.6,4X,'SUMP1=',E13.6,4X,'ERORH=',E10.3,
C      1        4X,'HI2=',E13.6,4X,'SUMH2=',E13.6)
C      MAIN0331
AA=BB      MAIN0332
IF (EROPP.LT.10.E-05.AND.ERORH.LT.10.E-05) GO TO 800      MAIN0333
650 CCNTINUE      MAIN0334
800 CCNTINUE      MAIN0335
C      MAIN0336
PI1=SUMP1      MAIN0337
PI2=SUMP2      MAIN0338
HI1=SUMH1      MAIN0339
HI2=SUMH2      MAIN0340
C      MAIN0341
*****      MAIN0342
*   TAU>0. : INTEGRATION FROM K4 TO INFINITY *      MAIN0343
*****      MAIN0344
C      MAIN0345
*****      MAIN0346
C      MAIN0347
SUMP1=0.      MAIN0348
SUMP2=0.      MAIN0349
SUMH1=0.      MAIN0350
SUMH2=0.      MAIN0351
AA=0.      MAIN0352
C      MAIN0353
DC 850 ITER=1,NT,2      MAIN0354
C      MAIN0355
CALL ROOT (ITER,ETAU,ANU,F)      MAIN0356
C      MAIN0357
IF (RCOTR(1).GT.RK4.AND.RCOTT(1).EQ.0.) CXX=RCOTR(1)      MAIN0358
IF (RCOTR(2).GT.RK4.AND.RCOTT(2).EQ.0.) CXX=RCOTR(2)      MAIN0359
IF (RCOTR(3).GT.RK4.AND.RCOTT(3).EQ.0.) CXX=RCOTT(3)      MAIN0360
IF (RCOTR(4).GT.RK4.AND.RCOTT(4).EQ.0.) CXX=RCOTR(4)

```

**COPY AVAILABLE TO DDC DOES NOT  
PERMIT FULLY LEGIBLE PRODUCTION**

```

C          EE=SORT (CXX-RK4)           MAIN0361
          XIN=EE-AA                 MAIN0362
C
C.....INTERMEDIATE RESULTS CAN BE PRINTED IF DESIRED   MAIN0363
C          WRITE (M,40) IITER            MAIN0364
C          40 FFORMAT (8X,'ITER=',I3/)    MAIN0365
C          WRITE (M,41) (ROOTR(I2),I2=1,4), (RCOII(I2),I2=1,4)  MAIN0366
C          41 FFORMAT (8X,'R1=',E13.6,5X,'R2=',E13.6,5X,'R3=',E13.6,5X,'R4=',  MAIN0367
C          1 E13.6/8X,'I1=',E13.6,5X,'I2=',E13.6,5X,'I3=',E13.6,5X,'I4=',  MAIN0368
C          2 E13.6/)                  MAIN0369
C          WRITE (M,42) AA,BB,CXX        MAIN0370
C          42 FFORMAT (8X,'AA=',E13.6,4X,'BB=',E13.6,4X,'CXX=',E13.6/)  MAIN0371
C
C          PI1=0.                     MAIN0372
C          PI2=0.                     MAIN0373
C          HI1=0.                     MAIN0374
C          HI2=0.                     MAIN0375
C
C.....10-POINT GAUSS-LEGENDRE QUADRATURE FOR A GIVEN INTERVAL  MAIN0376
C          DO 900 J4=1,10             MAIN0377
C          XKBAR=(XIN*Z(J4)+AA+BB)/2.  MAIN0378
C          WI=WEIT(J4)               MAIN0379
C          AKI=RK4*XKBAR**2           MAIN0380
C          IF (ITAU.F0.3) GO TO 910  MAIN0381
C          Z1=BTAU**2*SQRT((AKI-RK1)*(AKI-RK2)*(AKI-RK3))  MAIN0382
C          GC TO 920                MAIN0383
C          910 Z1=BTAU*SQRT(((BTAN*AKI-1.)**2+AKI)*(AKI-RK3))  MAIN0384
C          920 Z2=(BTAN*AKI-1.)*4        MAIN0385
C
C          SGN=1.                   MAIN0386
C          SGNX=BTAN*AKI-1.          MAIN0387
C          IF (SGNX.LT.0.) SGN=-1.  MAIN0388
C
C          Z3=Z2-AKI**2             MAIN0389
C          IF (Z3.LT.0.) Z3=0.       MAIN0390
C          Z4=COS(2.*XIN*B*SQRT(Z3))  MAIN0391
C          Z21=Z2*SGN/21            MAIN0392
C          Z22=Z21*(2.*Z4+2.)       MAIN0393
C
C          CALL T1Q1 (GT1,AKI,BTAU,FREQ,BPQ)  MAIN0394
C
C          E11=PI1*XIN*WI*PPO*Z21  MAIN0395
C          E12=PI2*XIN*WI*PPO*Z22  MAIN0396
C          H11=HI1*XIN*WI*HPO*Z21  MAIN0397
C          H12=HI2*XIN*WI*HPO*Z22  MAIN0398
C          900 CONTINUE               MAIN0399
C
C          SUMP1=SUMP1+PI1            MAIN0400
C          SUMP2=SUMP2+PI2            MAIN0401
C          SUMH1=SUMH1+HI1            MAIN0402
C          SUMH2=SUMH2+HI2            MAIN0403
C
C          ERORP=AES(PI1/SUMP1)      MAIN0404
C          ERORH=AES(HI1/SUMH1)      MAIN0405
C
C.....INTERMEDIATE RESULTS CAN BE PRINTED IF DESIRED   MAIN0406
C          WRITE (M,50) PI1,SUMP1,ERORP,PI2,SUMP2  MAIN0407
C          50 FFORMAT (8X,'PI1=',E13.6,4X,'SUMP1=',E13.6,4X,'ERORP=',E10.3,  MAIN0408
C          1 4X,'PT2=',E13.6,4X,'SUMP2=',E13.6/)  MAIN0409
C          WRITE (M,51) HI1,SUMH1,ERORH,HI2,SUMH2  MAIN0410
C          51 FFORMAT (8X,'HI1=',E13.6,4X,'SUMH1=',E13.6,4X,'ERORH=',E10.3,  MAIN0411
C          1 4X,'HI2=',E13.6,4X,'SUMH2=',E13.6/)  MAIN0412
C
C          AA=EP
C          IF (ERORP.LT.10.E-05.AND.ERORH.LT.10.E-05) GC TO 950  MAIN0413
C          850 CONTINUE
C          950 CONTINUE
C
C          E1T3=SUMP1                MAIN0414
C          P213=SUMP2                MAIN0415
C          H1T3=SUMH1                MAIN0416
C
C.....INTERMEDIATE RESULTS CAN BE PRINTED IF DESIRED   MAIN0417
C          WRITE (M,52) PI1,SUMP1,ERORP,PI2,SUMP2  MAIN0418
C          52 FFORMAT (8X,'PI1=',E13.6,4X,'SUMP1=',E13.6,4X,'ERORP=',E10.3,  MAIN0419
C          1 4X,'PT2=',E13.6,4X,'SUMP2=',E13.6/)  MAIN0420
C          WRITE (M,53) HI1,SUMH1,ERORH,HI2,SUMH2  MAIN0421
C          53 FFORMAT (8X,'HI1=',E13.6,4X,'SUMH1=',E13.6,4X,'ERORH=',E10.3,  MAIN0422
C          1 4X,'HI2=',E13.6,4X,'SUMH2=',E13.6/)  MAIN0423
C
C          AA=EP
C          IF (ERORP.LT.10.E-05.AND.ERORH.LT.10.E-05) GC TO 950  MAIN0424
C          850 CONTINUE
C          950 CONTINUE
C
C          E1T3=SUMP1                MAIN0425
C          P213=SUMP2                MAIN0426
C          H1T3=SUMH1                MAIN0427
C
C.....INTERMEDIATE RESULTS CAN BE PRINTED IF DESIRED   MAIN0428
C          WRITE (M,54) PI1,SUMP1,ERORP,PI2,SUMP2  MAIN0429
C          54 FFORMAT (8X,'PI1=',E13.6,4X,'SUMP1=',E13.6,4X,'ERORP=',E10.3,  MAIN0430
C          1 4X,'PT2=',E13.6,4X,'SUMP2=',E13.6/)  MAIN0431
C          WRITE (M,55) HI1,SUMH1,ERORH,HI2,SUMH2  MAIN0432
C          55 FFORMAT (8X,'HI1=',E13.6,4X,'SUMH1=',E13.6,4X,'ERORH=',E10.3,  MAIN0433
C          1 4X,'HI2=',E13.6,4X,'SUMH2=',E13.6/)  MAIN0434

```

```

C     82I3=SUMH2          MAIN0433
C
C     DF1 (J) = ((P1I1+P1I2+P1I3)*(-2.*WN*ANU/PI))/PNON  MAIN0434
C     DH1 (J) = ((H1I1+H1I2+H1I3)*(-2.*WN*ANU/PI))/HNCH  MAIN0435
C     DE2 (J) = ((F2I1+P2I2+P2I3)*(-WN*ANU/PI))/PNON    MAIN0436
C     DH2 (J) = ((H2I1+H2I2+H2I3)*(-WN*ANU/PI))/HNON    MAIN0437
C
C     410 CCNTINUE        MAIN0438
C     250 CCNTINUE        MAIN0439
C           WRITE (M,52) (OM(J),DF1(J),DP2(J),DH1(J),DH2(J),J=1,NOM)  MAIN0440
C     52  FORMAT (//5X,'CMEGA',1CX,'DP1',13X,'DP2',13X,'DH1',13X,'DH2'//  MAIN0441
C           (5X,P5.3,1X,4E16.5))  MAIN0442
C     200 CCNTINUE        MAIN0443
C           STOP            MAIN0444
C           END             MAIN0445

```

```

SUBROUTINE PIOI(AK,RNC,TAU,FPO,HPO)
COMMON /GEOM/ NSI,NSI,EFS(40),R(40),TC(40),X(40)
E1=0.
E2=0.
Q1=0.
Q2=0.
C
C     DC 1 I=1,NSI
C.....NSI IS THE NO. OF THE INTEGRATION INTERVAL(NSI=NST-1)
J=I+1
EPS1=EPS(I)
EPS2=EPS(J)
R1=R(I)
R2=R(J)
TC1=TC(I)
TC2=TC(J)
HH1=SQR1(E1**2-EPS1**2)
HH2=SQR1(P2**2-EPS2**2)
H1=TO1-HH1
H2=TO2-HH2
X1=X(I)
X2=X(J)
DELX=X2-X1
EE=BNU*(TAU*AK-1.)**2
EDC=DC*EE
ENUK=BNU*PK
C
XX1=NUK*X1
XX2=BNUK*X2
C
CALL ZFIIN (DD,EPS1,TC1,R1,Z1)
CALL ZETIN (DD,EPS2,TC2,R2,Z2)
C
CALL ZETINS (DD,EPS1,TC1,R1,H1,ZS1)
CALL ZETINS (DD,EPS2,TC2,R2,H2,ZS2)
C
PIQI0001
PIQI0002
PIQI0003
PIQI0004
PIQI0005
PIQI0006
PIQI0007
PIQI0008
PIQI0009
PIQI0010
PIQI0011
PIQI0012
PIQI0013
PIQI0014
PIQI0015
PIQI0016
PIQI0017
PIQI0018
PIQI0019
PIQI0020
PIQI0021
PIQI0022
PIQI0023
PIQI0024
PIQI0025
PIQI0026
PIQI0027
PIQI0028
PIQI0029
PIQI0030
PIQI0031
PIQI0032
PIQI0033
PIQI0034
PIQI0035
PIQI0036

```

```

        W1=-R1*CD          PIQI0037
        W2=-R2*CD          PIQI0038
C       IF (WW1.LT.-50.) EP1=0.          PIQI0039
C       IF (WW1.LT.-50.) GO TO 10          PIQI0040
C       EE1=EXP(WW1)          PIQI0041
C
 10    IF (WW2.LT.-50.) EP2=0.          PIQI0042
C       IF (WW2.LT.-50.) GO TO 20          PIQI0043
C       EE2=EXP(WW2)          PIQI0044
C
 20    CONTINUE          PIQI0045
C
C       PH1=EPS1*EP1-Z1          PIQI0046
C       PH2=EPS2*EP2-Z2          PIQI0047
C
C       PPA1=ZS1          PIQI0048
C       PPA2=ZS2          PIQI0049
C
C       AA1=(-WW1+1.)/DDD *EE1-(1./DDD)          PIQI0050
C       AA2=(-WW2+1.)/DDD *EE2-(1./DDD)          PIQI0051
C       PEB1=EPS1*AA1          PIQI0052
C       PEE2=EPS2*AA2          PIQI0053
C
C       FPC1=X1*FH1          PIQI0054
C       FPC2=X2*FF2          PIQI0055
C
C       APAI=(PPA2-PPA1)/DELX          PIQI0056
C       APBI=(PPE2-PPE1)/DELX          PIQI0057
C       APC1=(PFC2-PFC1)/DELX          PIQI0058
C
C       BEAI=PPA1-APAI*X1          PIQI0059
C       BEBI=PPE1-APBI*X1          PIQI0060
C       EFC1=PFC1-APCI*X1          PIQI0061
C
C       IF (BNUK.EQ.0.) GO TO 50          PIQI0062
C
C       FFS1=(FC(XX2)-PC(XX1))/ENUK          PIQI0063
C       FFC1=(FS(XX2)-PS(YY1))/ENUK          PIQI0064
C
C       FS1=SIN(YY2)-SIN(YY1)          PIQI0065
C       FCC1=COS(YX1)-COS(XX2)          PIQI0066
C
C       FFS2=(PS(XX2)-PS(XX1))/ENUK**2          PIQI0067
C       FCC2=(FC(XX2)-FC(XX1))/ENUK**2          PIQI0068
C
C       FSS2=(COS(XX1)-COS(XX2))/BNUK          PIQI0069
C       FCC2=(SIN(XX2)-SIN(XX1))/ENUK          PIQI0070
C
C       AHI=(RH2-RH1)/DRLX          PIQI0071
C       BET=PH1-AHI*X1          PIQI0072
C
C       EE1=-((APAI+APBI)*PPS1+(PPA1+PPB1)*FSS1)          PIQI0073
C       1      -(APCI*PPS2+PPC1*FSS2)          PIQI0074
C       CC1=-(PPI+APPI)*PPC1+(PPI+EPPI)*FCC1          PIQI0075
C       1      -(APCI*PPC2+PPC1*FCC2)          PIQI0076
C       EE2=AHI*FES2+PH1*FSS2          PIQI0077
C       CC2=AHI*FCC2+PH1*PPC2          PIQI0078
C
C       P1=P1+PP1          PIQI0079
C       Q1=Q1+QC1          PIQI0080
C       E2=E2+PE2          PIQI0081
C       Q2=Q2+QC2          PIQI0082
C
C       GO TO 1          PIQI0083
C
 50    CONTINUE          PIQI0084
C
C.....CASE FOR ENUK=0.
C       E1=E2=0.          PIQI0085
C       Q1=Q1-(PPC1+PPC2)*DEIX/2.          PIQI0086
C       Q2=Q2+(RH1+RH2)*DEIX/2.          PIQI0087
C
C
 1    CONTINUE          PIQI0088

```

```

C          PIQI0109
PFO=P1**2+Q1**2          PIQI0110
HEQ=P2**2+Q2**2          PIQI0111
C          PIQI0112
      RETURN          PIQI0113
      END          PIQI0114

```

```

SUBROUTINE ZETIN(DD,FPS,T,R,Z)
IF(R.EQ.0.) Z=0.
IF(R.EQ.C.) RETURN
NUM=10
DIV=2.*PICAT(NUM)
A=EPS/R
GAMMA=2.
ALPA=PSIN(A)
E=R*COS(ALPA)
TA=P-T
TE=-T-R
C.... F,T ARE POSITIVE ( THE RADIUS AND DEPTH TO THE AXIS)
H=(TA-TE)/DIV
X=TB
Z=0.
DO 1 I=1,NUM
XB=X+H
XHH=X+2.*H
Z=Z+PI/3.* (P(DD,T,R,X)+4.*F(DD,T,R,XB)+P(DD,T,R,XHH))
1 X=X+2.*H
Z=GAMMA*Z*DD
RETURN
END

```

ZETN0001  
 ZETN0002  
 ZETN0003  
 ZETN0004  
 ZETN0005  
 ZETN0006  
 ZETN0007  
 ZETN0008  
 ZETN0009  
 ZETN0010  
 ZETN0011  
 ZETN0012  
 ZETN0013  
 ZETN0014  
 ZETN0015  
 ZETN0016  
 ZETN0017  
 ZETN0018  
 ZETN0019  
 ZETN0020  
 ZETN0021  
 ZETN0022  
 ZETN0023

```

C          ZTNS0001
SUBROUTINE ZTINS(DD,FES,TO,R,H,ZS)
EE=NU*(TAU+K-1)**2          ZTNS0002
IF (R.EQ.0.) ZS=0.
IF (R.EQ.C.) RETURN          ZTNS0003
N=10
DIV=2.*FICAT(N)
T=TO+F
F=(T-H)/DIV
C.... 'E' IS THE SPACING OF THE INTEGRATION
X=-T
ZS=0.
C          ZTNS0004
DO 1 I=1,N
XE=X+E
XEB=X+2.*E
ZS=ZS+T/3.* (S(DD,TO,R,X)+4.*S(DD,TO,R,XB)+S(DD,TO,R,XEE))
1 X=X+2.*E
C          ZTNS0005
      RETURN          ZTNS0006
      END          ZTNS0007

```

ZTNS0008  
 ZTNS0009  
 ZTNS0010  
 ZTNS0011  
 ZTNS0012  
 ZTNS0013  
 ZTNS0014  
 ZTNS0015  
 ZTNS0016  
 ZTNS0017  
 ZTNS0018  
 ZTNS0019  
 ZTNS0020

```

SUBROUTINE RCOT(ITER,TAU,ANU,YDIS)
DIMENSION XC0F(5),COF(5)
COMMON/CNE/ROCTR(4),RCCTI(4)
MM=4
PI=3.14159
XET=PI*FLCAT(ITER)
A=-4./TAU
B=6./TAU**2-1./TAU**4
C=-4./TAU**3
DD=XPI/(2.*ANU*YDIS)
D=(1.-DD*ED)/TAU**4
XC0F(1)=C
XC0F(2)=C
XC0F(3)=E
XC0F(4)=A
XC0F(5)=1.
CALL PCIR(XC0F,COF,MM,RCOTR,RCCTI,IER)
RETURN
END

```

```

ROOT0001
ROOT0002
ROOT0003
ROOT0004
ROOT0005
ROOT0006
ROOT0007
ROOT0008
ROOT0009
ROOT0010
ROOT0011
ROOT0012
ROOT0013
ROOT0014
ROOT0015
ROOT0016
ROOT0017
ROOT0018
ROOT0019

```

```

FUNCTION F(D,T,R,X)
A=T+X
AA=A*A
EE=D*D-AA
EE=SQRT(EE)
B=SQRT(EE)
A1=D*X
A2=-A1
IF(A2.GT.50.) F=0.
IF(A2.GT.50.) RETURN
F=B*EXP(A1)
RETURN
END
FUNCTION S(EE,TC,R,ZFIN)
A=ZETA+TC
ARG=AES(R*R-A*A)
C.....'R' IS LESS THAN OR EQUAL TO 'A', BUT DUE TO THE SLIGHT
C.....NUMERICAL ERROR, R*R-A*A SOMETIMES GIVES '-' VALUES, THUS
C.....TAKING THE ABS(R*R-A*A) IS PREFERRED.
H=SORT(ARG)
AA=DD*ZETA
C
IF (AA.LT.-50.) S=0.
IF (AA.LT.-50.) RETURN
C
S=H*ZETA*EXP(AA)
RETURN
END

```

```

FNC10001
FNC10002
FNC10003
FNC10004
FNC10005
FNC10006
FNC10007
FNC10008
FNC10009
FNC10010
FNC10011
FNC10012
FNC10013
FNC10014
FNC10015
FNC10016
FNC10017
FNC10018
FNC10019
FNC10020
FNC10021
FNC10022
FNC10023
FNC10024
FNC10025
FNC10026
FNC10027
FNC10028

```

```

FUNCTION FS(X)          FNC20001
A=SIN(X)                FNC20002
E=X*COS(X)              FNC20003
FS=A-E                  FNC20004
RETURN                   FNC20005
END                      FNC20006
FUNCTION FC(X)          FNC20007
A=COS(X)                FNC20008
B=X*SIN(X)              FNC20009
FC=A+B                  FNC20010
RETURN                   FNC20011
END                      FNC20012
FUNCTION SS(EPS,TO,RC)  FNC20013
PI=3.1415926            FNC20014
IF(RO.FC.C.) SS=0.        FNC20015
IF(RO.FC.O.) RETURN      FNC20016
ALPA=ASIN(EPS/RC)        FNC20017
B=RO*COS(ALPA)          FNC20018
BE=B/2.                  FNC20019
A1=2.*EPS*(TC-FF)        FNC20020
A2=RO**2*(PI-ALPA)       FNC20021
SS=A1+A2                 FNC20022
RETURN                   FNC20023
END                      FNC20024
FUNCTION ASIN(X)         FNC20025
A=SQRT(1.-X*X)           FNC20026
E=X/A                   FNC20027
ASIN=ATAN(B)             FNC20028
RETURN                   FNC20029
END                      FNC20030

```

# COPY AVAILABLE TO DDCI DOES NOT PERMIT FULLY LEGIBLE PRODUCTION

November 1973

DISTRIBUTION LIST FOR UNCLASSIFIED  
TECHNICAL REPORTS ISSUED UNDER

CONTRACT N604-67-A-0047-CDA-1 TASK AF-67-A-0047-CDA-1

All addressees receive one copy unless otherwise specified

- Defense Documentation Center  
Cameron Station  
Alexandria, VA 22314      12 copies
- Technical Library  
Naval Ship Research & Dev. Center  
Annapolis Laboratory  
Annapolis, MD 21402
- Professor Bruce Johnson  
Engineering Department  
Naval Academy  
Annapolis, MD 21402
- Library  
Naval Academy  
Annapolis, MD 21402
- Professor C. S. Yih  
Department of Engineering Mechanics  
University of Michigan  
Ann Arbor, MI 48108
- Professor W. P. Graebel  
Department of Engineering Mechanics  
University of Michigan  
Ann Arbor, MI 48108
- Professor T. Francis Ogilvie  
Department of Naval Architecture  
and Marine Engineering  
University of Michigan  
Ann Arbor, MI 48108
- Professor W. V. Willmarth  
Department of Aerospace Engineering  
University of Michigan  
Ann Arbor, MI 48108
- Professor R. B. Couch  
Department of Naval Architecture  
and Marine Engineering  
University of Michigan  
Ann Arbor, MI 48108
- Air Force Office of Scientific  
Research (REX)  
1400 Wilson Boulevard  
Arlington, VA 22209
- Defense Documentation Center  
Cameron Station  
Alexandria, VA 22314      12 copies
- Technical Library  
Naval Ship Research Corporation  
Northway 10 Executive Park  
Ballston Lake, NY 12019
- Professor S. Corrsin  
Department of Mechanics and  
Materials Sciences  
The Johns Hopkins University  
Charles and 34th Street  
Baltimore, MD 21218
- Professor L. S. G. Kovasznay  
Department of Mechanics and Materials  
Sciences  
The Johns Hopkins University  
Charles and 34th Street  
Baltimore, MD 21218
- Commander  
Puget Sound Naval Shipyard  
Bremerton, WA 98334
- Dr. Edward E. Felt  
Commander  
Fleet Ballistic Missile Division  
Fleet Ballistic Missile Division  
Buffalo, NY 14221
- Professor M. Holt  
Department of Mechanical Engineering  
University of California  
Berkeley, CA 94720
- Professor E. V. Laittone  
Department of Mechanical Engineering  
University of California  
Berkeley, CA 94720
- Librarian  
Department of Naval Architecture  
University of California  
Berkeley, CA 94720
- Professor P. Lieber  
Department of Mechanical Engineering  
University of California  
Berkeley, CA 94720
- Professor J. R. Paulling  
Department of Naval Architecture  
University of California  
Berkeley, CA 94720
- Professor C. C. Mei  
Department of Civil Engineering  
Massachusetts Institute of Technology  
Cambridge, MA 02139
- Professor Phillip Vandell  
Department of Ocean Engineering  
Massachusetts Institute of Technology  
Cambridge, MA 02139
- Professor J. V. Wehausen  
Department of Naval Architecture  
University of California  
Berkeley, CA 94720
- Professor J. A. Schetz  
Department of Aerospace Engineering  
Virginia Polytechnic Institute  
Blacksburg, VA 24061
- Director  
Office of Naval Research Branch Office  
195 Summer Street  
Boston, MA 02210
- Professor L. M. Howard  
Department of Mathematics  
Massachusetts Institute of Technology  
Cambridge, MA 02139
- Professor R. P. Probstein  
Department of Mechanical Engineering  
Massachusetts Institute of Technology  
Cambridge, MA 02139
- Professor E. Mollo-Christensen  
Department of Meteorology  
Massachusetts Institute of Technology  
Cambridge, MA 02139
- Professor J. Nicholas Newman  
Department of Ocean Engineering  
FOC 5-1024  
Massachusetts Institute of Technology  
Cambridge, MA 02139
- Professor A. P. Kuhlmey, Director  
Research Laboratories for the Engineering  
Sciences  
Thornton Hall  
University of Virginia  
Charlottesville, VA 22903
- Director  
Office of Naval Research Branch Office  
526 South Clark Street  
Chicago, IL 60605
- Library  
Naval Weapons Center  
China Lake, CA 93555
- Institute of Hydrodynamics and Hydraulic  
Engineering  
Technical University of Denmark  
Building 315, DK-2800 Copenhagen, Denmark
- Professor M. A. Arkowitz  
Department of Ocean Engineering  
Massachusetts Institute of Technology  
Cambridge, MA 02139
- Professor H. A. Krebs  
Department of Naval Architecture  
Massachusetts Institute of Technology  
Cambridge, MA 02139

Page 1

- Professor E. Restivo  
Division of Chemical Engineering  
Science  
Case Western Reserve University  
Cleveland, OH 44106
- Professor J. M. Burgers  
Institute of Fluid Dynamics and  
Applied Mathematics  
University of Maryland  
College Park, MD 20742
- Professor Paul  
Institute for Fluid Dynamics and  
Applied Mathematics  
University of Maryland  
College Park, MD 20740
- Acquisitions Branch (S-AM/DL)  
NASA Scientific and Technical  
Information Facility  
P. O. Box 33  
College Park, MD 20740
- Technical Library  
Naval Weapons Laboratory  
Dahlgren, VA 22443
- Dr. C. S. Wells, Jr.  
Advanced Technology Center, Inc.  
P. O. Box 614  
Dallas, TX 75222
- Dr. R. H. Erickson  
Dublin, NH 03444
- Airway Research Office  
Box CN, Duke Station  
Durham, NC 27716
- Dr. Martin H. Bloom  
Polytechnic Institute of New York  
Department of Aerospace Engineering  
and Applied Mechanics  
Poughkeepsie, NY 12533
- Technical Documents Center  
Army Mobility Equipment R&D Center  
Fort Belvoir, VA 22060

Page 4

- Professor J. E. Gersak  
Department of Civil Engineering  
Fluid Mechanics Program  
Colorado State University  
Fort Collins, CO 80523.
- Professor O. H. Shemdin  
Coastal and Oceanographic Engineering  
Department  
University of Florida  
Gainesville, FL 32601
- Technical Library  
Webb Institute of Naval Architecture  
Glen Cove, NY 11542
- Professor E. V. Lewis  
Webb Institute of Naval Architecture  
Glen Cove, NY 11542
- Dr. M. Poroh  
Technion-Israel Institute of Technology  
Department of Civil Engineering  
Haifa, Israel
- Dr. J. P. Breslin  
Davidson Laboratory  
Stevens Institute of Technology  
Castile Point Station  
Hoboken, NJ 07030
- Mr. C. H. Henry  
Stevens Institute of Technology  
Castile Point Station  
Hoboken, NJ 07030
- Dr. D. Savitry  
Davidson Laboratory  
Stevens Institute of Technology  
Castile Point Station  
Hoboken, NJ 07030
- Dr. A. Scrimpf  
Davidson Laboratory  
Stevens Institute of Technology  
Castile Point Station  
Hoboken, NJ 07030
- Dr. J. P. Craven  
University of Hawaii  
1801 University Avenue  
Honolulu, HI 96822
- Mr. Phillip Eisenberg, President  
Hydrodynamics, Incorporated  
7210 Finsell School Road  
Laurel, MD 20610
- Mr. M. P. Mullin  
Hydrodynamics, Incorporated  
7210 Finsell School Road  
Laurel, MD 20610
- Commander  
Long Beach Naval Shipyard  
Long Beach, CA 90801
- Dr. C. W. Hirt  
University of California  
Los Alamos Scientific Laboratory  
P. O. Box 1653  
Los Alamos, NM 87544
- Professor John Laufer  
Department of Aerospace Engineering  
University of Southern California  
University Park  
Los Angeles, CA 90007
- Professor J. M. Killen  
St. Anthony Falls Hydraulic Laboratory  
University of Minnesota  
Minneapolis, MN 55414
- Lorenz G. Straub Library  
St. Anthony Falls Hydraulic Laboratory  
University of Minnesota  
Minneapolis, MN 55414
- Professor J. W. Miles  
Flow Research, Inc.  
1819 South Central Avenue  
Suite 72  
Kent, WA 98031
- Professor J. W. Miles  
Institute of Geophysics and  
Planetary Physics  
University of California, San Diego  
La Jolla, CA 92093
- Director  
Scripps Institute of Oceanography  
University of California  
La Jolla, CA 92093
- Professor A. M. Ellis  
Department of Applied Mathematics and  
Engineering Sciences  
University of California, San Diego  
La Jolla, CA 92093
- Dr. E. Salberman  
St. Anthony Falls Hydraulic Laboratory  
University of Minnesota  
Minneapolis, MN 55414
- Library  
Naval Postgraduate School  
Monterey, CA 93940
- Professor A. B. Metzner  
Department of Chemical Engineering  
University of Delaware  
Newark, DE 19711

# COPY AVAILABLE TO DDC DOES NOT DEPART FROM LEGAL PRODUCTION

PAGE 5

Technical Library  
Naval Underwater Systems Center  
Newport, RI 02840

Office of Naval Research  
New York Area Office  
207 W. 26th Street  
New York, NY 10011

Professor V. Castelli  
Department of Mechanical Engineering  
Columbia University  
New York, NY 10027

Professor H. G. Elrod  
Department of Mechanical Engineering  
Columbia University  
New York, NY 10027

Professor J. J. Stoker  
Courant Institute of Mathematical  
Sciences

New York University  
251 Mercer Street  
New York, NY 10003

Society of Naval Architects and  
Marine Engineers  
7b Trinity Place  
New York, NY 10006

Librarian, Aerautical Laboratory  
National Research Council  
Montreal Road  
Ottawa 7, Canada

Technical Library  
Naval Coastal System Laboratory  
Panama City, FL 32401

Dr. Jack W. Hoyt  
Code 2501  
Naval Undersea Center  
San Diego, CA 92132

Technical Library  
Naval Undersea Center  
Panama Laboratory  
3202 E. Foothill Blvd.  
Panama, CA 91107

Professor A. J. Acosta  
Department of Mechanical Engineering  
California Institute of Technology  
Pasadena, CA 91109

Professor H. W. Liepmann  
Graduate Aeronautical Laboratories  
California Institute of Technology  
Pasadena, CA 91109

Professor M. S. Plesset  
Engineering Science Department  
California Institute of Technology  
Pasadena, CA 91109

Professor A. Postko  
Graduate Aeronautical Laboratories  
California Institute of Technology  
Pasadena, CA 91109

Professor T. Y. Wu  
Engineering Science Department  
California Institute of Technology  
Pasadena, CA 91109

Director  
Office of Naval Research Branch Office  
1030 E. Green Street  
Pasadena, CA 91101

Professor K. M. Agrawal  
Virginia State College  
Department of Mathematics  
Petersburg, VA 23803

Technical Library  
Naval Ship Engineering Center  
Philadelphia Division  
Philadelphia, PA 19112

Technical Library  
Philadelphia Naval Shipyard  
Philadelphia, PA 19112

Professor C. E. Pearson  
Aerospace Research Laboratory  
University of Washington  
Seattle, WA 98105

Professor Bruce H. Adee  
Department of Mechanical Engineering  
University of Washington  
Seattle, WA 98195

Dr. Paul Kaplan  
Oceans Inc.  
Technical Industrial Park  
Plainview, NY 11803

Technical Library  
Naval Missile Center  
Point Loma, CA 92131

Commander  
Portsmouth Naval Shipyard  
Portsmouth, NH 03801

Commander  
Norfolk Naval Shipyard  
Portsmouth, VA 23709

Dr. H. Norman Abramson  
Southwest Research Institute  
8500 Culebra Road  
San Antonio, TX 78228

Editor  
Applied Mechanics Review  
Southeast Research Institute  
8500 Callebra Road  
San Antonio, TX 78206

Dr. Andrew Fabula  
Code 500, Building 106  
Naval Undersea Center  
San Diego, CA 92122

Office of Naval Research  
San Francisco Area Office  
760 Market Street, Room 417  
San Francisco, CA 94102

Librarian  
Pearl Harbor Naval Shipyard  
Box 100  
FPO San Francisco 96610

Technical Library  
Hunters Point Naval Shipyard  
San Francisco, CA 94135

Professor R. C. Dittma  
Pennsylvanian Polytechnic Institute  
Troy, NY 12181

Professor R. C. Petter  
Geophysical Fluid Dynamics Institute  
Tallahassee, FL 32306

Professor R. C. Seeger  
Department of Mathematics  
Pennsylvanian Polytechnic Institute  
Troy, NY 12181

Professor A. Hertzberg  
Director, Aerospace Research Laboratory  
University of Washington  
Seattle, WA 98105

Tenton Kennedy Document Library  
The Johns Hopkins University  
Applied Physics Laboratory  
8622 Georgia Avenue  
Silver Spring, MD 20910

Professor E. Y. Hsu  
Department of Civil Engineering  
Stanford University  
Stanford, CA 94305

Dr. Byrne Perry  
Department of Civil Engineering  
Stanford University  
Stanford, CA 94305

Dr. R. L. Street  
Department of Civil Engineering  
Stanford University  
Stanford, CA 94305

Professor Milton van Dyke  
Department of Aeronautical Engineering  
Stanford University  
Stanford, CA 94305

Professor R. Pfeiffer  
Florida State University  
Tallahassee, FL 32306

Professor R. C. Dittma  
Pennsylvanian Polytechnic Institute  
Troy, NY 12181

Professor J. W. Hall  
The Pennsylvania State University  
University Park, PA 16801

**Professor J. L. Lumley**  
Department of Aerospace Engineering  
Pennsylvania State University  
University Park, PA 16802

**Dr. J. M. Robertson**  
Department of Theoretical and  
Applied Mechanics  
University of Illinois  
Urbana, IL 61803

**Technical Library**  
Mare Island Naval Shipyard  
Vallejo, CA 94592

**Mr. Norman Kilsen**(SP 2022)  
Strategic Systems Project  
Office  
Department of the Navy  
Washington, DC 20376

**Office of Naval Research**  
Code 438  
800 N. Quincy Street  
Arlington, VA 22217

**Office of Naval Research**  
Code 438-7  
800 N. Quincy Street  
Arlington, VA 22217

**Office of Naval Research**  
Code 438-8  
800 N. Quincy Street  
Arlington, VA 22217

**Office of Naval Research**  
Code 438-9  
800 N. Quincy Street  
Arlington, VA 22217

**Office of Naval Research**  
Code 438-10  
800 N. Quincy Street  
Arlington, VA 22217

**Office of Naval Research**  
Code 438-11  
800 N. Quincy Street  
Arlington, VA 22217

**Office of Naval Research**  
Code 438-12  
800 N. Quincy Street  
Arlington, VA 22217

**Office of Naval Research**  
Code 438-13  
800 N. Quincy Street  
Arlington, VA 22217

**Office of Naval Research**  
Code 438-14  
800 N. Quincy Street  
Arlington, VA 22217

**Office of Naval Research**  
Code 481  
800 N. Quincy Street  
Arlington, VA 22217

**Naval Research Laboratory**  
Code 2627  
Washington, DC 20375

**Naval Research Laboratory**  
Code 2629 (ORNL)  
Washington, DC 20375

**Naval Research Laboratory**  
Code 4000  
Washington, DC 20375

**Naval Research Laboratory**  
Code 8030  
Washington, DC 20375

**Naval Research Laboratory**  
Code 8040  
Washington, DC 20375

**Naval Ordnance Systems Command**  
Code 031  
800 N. Quincy Street  
Washington, DC 20362

**Naval Sea Systems Command**  
Code 0322 (L. Pritz)  
Washington, DC 20332

**Naval Sea Systems Command**  
Code 032 (J. Strobl)  
Washington, DC 20332

**Naval Sea Systems Command**  
Code 0905 (D. F. 20362  
Washington, DC 20362

**Naval Sea Systems Command**  
Code 0312 (T. Petre)  
Washington, D. C. 20362

**Naval Ship Engineering Center**  
Code 6034  
Center Building  
Prince George's Center  
Baltimore, MD 20782

**Naval Ship Engineering Center**  
Code 6101E  
Center Building  
Prince George's Center  
Baltimore, MD 20782

**Naval Ship Engineering Center**  
Code 6110  
Center Building  
Prince George's Center  
Baltimore, MD 20782

**Naval Ship Engineering Center**  
Code 6111  
Center Building  
Prince George's Center  
Baltimore, MD 20782

**Naval Ship Engineering Center**  
Code 6116  
Center Building  
Prince George's Center  
Baltimore, MD 20782

**Naval Ship Engineering Center**  
Code 6117  
Center Building  
Prince George's Center  
Baltimore, MD 20782

**Naval Ship Engineering Center**  
Code 6118  
Center Building  
Prince George's Center  
Baltimore, MD 20782

**Naval Ship Engineering Center**  
Code 6119  
Center Building  
Prince George's Center  
Baltimore, MD 20782

**Naval Ship Engineering Center**  
Code 6120  
Center Building  
Prince George's Center  
Baltimore, MD 20782

**Naval Ship Engineering Center**  
Code 6121  
Center Building  
Prince George's Center  
Baltimore, MD 20782

**Naval Ship Engineering Center**  
Code 6122  
Center Building  
Prince George's Center  
Baltimore, MD 20782

**Naval Ship Engineering Center**  
Code 6123  
Center Building  
Prince George's Center  
Baltimore, MD 20782

**Mr. J. B. Hadler**(Code 156)  
Naval Ship Research & Dev. Center  
Bethesda, MD 20034

**Mr. P. Fien**(Code 1521)  
Naval Ship Research & Dev. Center  
Bethesda, MD 20034

**Mr. Paul S. Granville**(Code 1511)  
Naval Ship Research & Dev. Center  
Bethesda, MD 20034

**Mr. J. McCarthy**(Code 1552)  
Naval Ship Research & Dev. Center  
Bethesda, MD 20034

**Mr. R. H. Salveter**(Code 1552)  
Naval Ship Research & Dev. Center  
Bethesda, MD 20034

**Ms. Joanne Scott**(Code 1813)  
Naval Ship Research & Dev. Center  
Bethesda, MD 20034

**Dr. A. Powell**(Code 01)  
Naval Ship Research & Dev. Center  
Bethesda, MD 20034

**Mr. W. M. Ellsworth**(Code 11)  
Naval Ship Research & Dev. Center  
Bethesda, MD 20034

**Mr. W. F. Cummins**(Code 15)  
Naval Ship Research & Dev. Center  
Bethesda, MD 20034

**Mr. G. H. Gleisner**(Code 18)  
Naval Ship Research & Dev. Center  
Bethesda, MD 20034

**Mr. R. Werner**(Code 152)  
Naval Ship Research & Dev. Center  
Bethesda, MD 20034

**Mr. W. B. Morgan**(Code 154)  
Naval Ship Research & Dev. Center  
Bethesda, MD 20034

**Naval Ordnance Systems Command**  
ORD 5413  
Washington, DC 20360

**Dr. G. Kulin**  
Fluid Mechanics Section  
National Bureau of Standards  
Washington, DC 20234

**Strategic Systems Project Office**

CNN (FNL-1)

Washington, DC 20360

**Oceanographer of the Navy**

200 Stovall Street

Alexandria, VA 22332

**Commander**

Naval Oceanographic Office

Washington, DC 20373

**Dr. A. L. Slafkosky**

Scientific Advisor

Commandant of the Marine Corps

(Code AX)

Washington, DC 20380

**Librarian Station 5-C**

Coast Guard Headquarters

NASMF Building

100 Seventh Street, S.W.

Washington, DC 20591

**Office of Research and Development**

Maritime Administration

441 G Street, N.W.

Washington, DC 20235

**Division of Ship Design**

Maritime Administration

441 G Street, N.W.

Washington, DC 20235

**National Science Foundation**

Engineering Division

1800 G Street, N.W.

Washington, DC 20550

**Science & Technology Division**

Library of Congress

Washington, DC 20540

**Chief of Research and Development**

Office of Chief of Staff

Department of the Army

Washington, DC 20310

**Professor A. Thiruvengadam**

Department of Mechanical Engineering

Catholic University of America

Washington, DC 20017

**Librarian**

Naval Ordnance Laboratory

White Oak, MD 20910

**Mr. J. Enig** (Room 3-252)

Naval Ordnance Laboratory

White Oak, MD 20910

**Dr. A. S. Tobrall, President**

General Technical Services, Inc.

451 Penn Street

Yeadon, PA 19050